Hydrol. Earth Syst. Sci. Discuss., doi:10.5194/hess-2016-507, 2016
Manuscript under review for journal Hydrol. Earth Syst. Sci.
Published: 28 November 2016

Simulations of water, heat, and solute transport in partially frozen soils

Mousong Wu[1,2], Per-Erik Jansson[2], Xiao Tan[1], Jiesheng Huang[1], Jingwei Wu[1]

1.State Key Laboratory of Water Resources and Hydropower Engineering Science, Wuhan University, 430072 Wuhan, Hubei, China

2.Department of Sustainable Development, Environmental Science and Engineering, KTH Royal Institute of Technology, 10044 Stockholm, Sweden

Abstract

Experiments for soil freezing/thawing were conducted in two seasonally frozen agricultural fields in northern China during 2011/2012 and 2012/2013 wintertime, respectively. Mass balance was checked based on measured data at various depths. Simulation work was conducted by combining CoupModel with Monte-Carlo sampling method to achieve parameter sets with equally good performance. Uncertainties existed in both measurements and model due to complexity in freezing/thawing processes as well as in surface energy partitioning. Parameters related to surface radiation and soil frost were strongly constrained with datasets available in two sites combining multi-criterion on outputs. Simulated soil heat processes were better described than soil water processes given the data obtained for calibration. Model performance was improved with consideration of solute effects on freezing point depression. More detailed solute transport processes in CoupModel needed to be improved by taking more processes such as diffusion and expulsion into consideration based on more precise experimental results, to reduce uncertainty in model. Generally, combination of measurement with process-based model and Monte-Carlo sampling method provided an approach for understanding of solute transport as well as its influences on soil freezing/thawing in cold arid agricultural regions. Incorporating more detailed descriptions of processes for frozen soil in the model can be justified if uncertainties in measurements can be reduced by introducing of high-precision novel technologies.

Keywords: Frozen soil; Solute; Uncertainty; Freezing point; Salinization

Correspondence author.
Email: jingwei.wu@whu.edu.cn

Hydrol. Earth Syst. Sci. Discuss., doi:10.5194/hess-2016-507, 2016
Manuscript under review for journal Hydrol. Earth Syst. Sci.
Published: 28 November 2016

1. Introduction

Soil freezing and thawing processes has long been recognized for its importance in not only engineering applications (e.g., construction of roads and pipelines) (Hansson *et al.*, 2004; Wettlaufer and Worster, 2006; Jones, 1981), but also environmental issues (e.g., soil erosion, flooding, and pollutants migration) (Seyfried and Murdock, 1997; Andersland *et al.*, 1996; Baker and Spaans, 1997; McCauley *et al.*, 2002). The investigation of soil freezing and thawing could result in a better understanding of water and solute distribution in soil (Baker and Osterkamp, 1989), frost heaving (Wettlaufer and Worster, 2006), waste disposal (McCauley *et al.*, 2002), climate change in cold regions (Lopez *et al.*, 2007).

Many experimental observations have been conducted since 1930s to study the freezing/thawing phenomenon in soil (Beskow, 1947; Edlefsen and Anderson, 1943; Spaans and Baker, 1996; Miller, 1980). For example, Beskow (1947) observed the accumulation of water towards freezing front and the influences of water, soil and solutes on freezing point depression, as well as the similarity between freezing and drying. Edlefsen and Anderson (1943) then formulated the relationship between soil temperature and freezing soil water potential by generalized Clausius-Clapeyron equation. Koopmans and Miller (1966) then tested the similarity between soil freezing curves and water retention curves. Burt and Williams (1976) measured hydraulic conductivity of freezing soil in laboratory, and this work was then put forward by others (Nakano *et al.*, 1982; Horiguchi and Miller, 1983; Black and Hardenberg, 1991). At the same time, formulation of the soil freezing/thawing processes has been raised up. e.g., the use of Clausius-Clapeyron equation for representation of soil freezing equilibrium (Kay and Groenevelt, 1974; Groenevelt and Kay, 1974), the power relationship between liquid water content and soil temperature (Anderson and Tice, 1973), the capillary bundle model for soil freezing characteristics (Watanabe and Flury, 2008; Lebeau and Konrad, 2012), and the influences of solute on soil freezing/thawing (Bing and Ma, 2011; Azmatch *et al.*, 2012; Wu *et al.*, 2015).

Laboratory and field experiments on soil freezing/thawing processes have received more attention. Watanabe *et al.* (2013) conducted laboratory experiments to describe the influence of soil freezing on infiltration. Zhou *et al.* (2014) measured the water content and ice content in a freezing soil column with gamma ray attenuation and TDR method. Also, field experiments were conducted to study plot-scale or regional water, heat and solute transport during freezing/thawing from different aspects. Radke and Berry (1998) analyzed the influences of soil water, bulk density as well as microbial activities on soil water and solute transport in the field soil column experiments. Stahli *et al.* (2004) characterized the preferential flow in frozen soil with dying method and proposed a two-domain model for flow in frozen soil. Iwata *et al.* (2008, 2010a, 2010b) studied the infiltration of snow melt under various controls as well the influences on water, heat dynamics in frozen soil, in the agricultural field in Japan. Parkin *et al.* (2013) studied the effects of tillage on freezing/thawing of agricultural field. Zhao *et al.* (2013) conducted field experiment to analyze influence of snowmelt infiltration on hydrological processes in winter in Inner Mongolia, China. Wu *et al.* (2016) studied the evaporation from seasonally frozen soil under various salt and groundwater conditions using field frost tube experiments, in Inner Mongolia, China. All these experiments demonstrated that water, heat and solute in frozen soil could be influenced by both soil conditions and boundary conditions, but due to a lot of uncertainties in experimental treatments as well in measurements, experimental studies on frozen soil could result in some uncertainties in knowledge of soil freezing/thawing.

Along with the experimental studies, numerical models have been put forward by many. The coupled water and heat transport model by Harlan (1973) considered the coupled relationship between water and heat in frozen soil. Then, Jame and Norum (1980) set up a finite element numerical model based on Harlan's model, and tested it with laboratory experimental results. This coupled model was then improved and tested by a lot of researchers with datasets from both laboratory and field (Mu and Ladanyi, 1987; Li *et al.*, 2000; Li *et al.*, 1998). All these models did not consider the transport of solute in frozen soil and neglected the influence of solutes on soil freezing. Flerchinger and Saxton (1989) proposed a simultaneous heat and water model for simulating water, heat and solute transport in frozen soil with snow and residue covering. Then this model was tested in many cold regions (Li *et al.*, 2012; Li *et al.*, 2013) and showed high flexibility in application under various conditions. Jansson and Karlberg (2004) developed a coupled process-based model based on the SOIL model to simulate water, heat as well solute transport in frozen soil. This model was verified in forests (Gustafsson *et al.*, 2004; Wu and Jansson, 2013), agricultural field (Wu *et al.*, 2011), permafrost (Zhang *et al.*, 2012; Scherler *et al.*, 2013) and other ecosystems (Khoshkhoo *et al.*, 2015). Hansson *et al.* (2004) also added a freezing module to one-dimensional water, heat and solute transport model HYDRUS, and tested the sensitivity of model using experimental results. Meanwhile, a lot of other models have taken soil freezing/thawing into consideration when applied to wintertime (e.g., SWAP, DRAINMOD, SWAT, HBV, VIC etc.). Numerical models have become a popular tool for understanding water, heat as well as solute transport in winter with complex boundary conditions and phase change.

However, there are large uncertainties in both experiments and models for soil freezing and thawing due to the complexity of phase change and coupled processes. For example, the measurement of liquid water content in frozen soil, the sampling of frozen soil, the measurements of hydraulic and thermal properties for frozen soil could be difficult due to limitations in technologies and in considering all effects on soil freezing/thawing (e.g., water, heat, solutes, soil textures as well as boundary conditions). Meanwhile, the setup of model always neglected some minor influences by taking the major one into consideration, e.g., the assumption of thermo-equilibrium of soil freezing, the neglecting of solute dispersion and expulsion in frozen soil, or even the neglecting of solute effects on freezing point depression, etc. All these would pose uncertainties to the study on soil freezing/thawing in natural conditions. To reduce uncertainties in both experiments and modeling, uncertainty analysis method is always used by combining experimental data with numerical model to calibrate the model for better representing reality. The generalized likelihood uncertainty estimation (GLUE) technique (Beven and Binley, 1992) is the commonly used method for uncertainty analysis in environmental modeling.

Instead of searching for an optimal parameter set, the GLUE method generates ensembles of parameter sets that show equally good performance in simulations (Candela *et al.*, 2005), as called 'equifinality' by Beven (2006). This method has been widely used in hydrologic simulations (Freer *et al.*, 1996; Beven and Freer, 2001; Liu *et al.*, 2009; Li *et al.*, 2010;Song *et al.*, 2015; Sun *et al.*, 2016) and climate change projections (Cameron *et al.*, 2000; Wilby, 2005; Choi and Beven, 2007; Bastola *et al.*, 2011; Lin *et al.*, 2015). There are only a few modeling work with agricultural water resources (Brazier *et al.*, 2000; Wang *et al.*, 2006; He *et al.*, 2010; Wu *et al.*, 2011; DeJonge *et al.*, 2012; Chisanga *et al.*, 2015).

In models for soil water, heat and solute transport (e.g., CoupModel, HYDRUS, SHAW), there are many parameters related to different coupled transport processes, also including non-linear responses , especially when considering soil freezing/thawing and solute transport. The parameters in these models are possible to measure with independent methods but those are big challenges because of high variability in the environments and many temporal and spatial scale related dependencies. Also, model structures are always simplified for description of some processes. Thus, for investigation of coupled processes in seasonally frozen agricultural field, it is important to use the GLUE method combining process-based model to unveil the freezing/thawing phenomenon.

In this study, we conducted field experiments on water, heat and solute transport in two sites in northern part of China. They are special both for the climates and the soils in cold regions in China. The coupled transport of water, heat and solute during wintertime is common for these two sites. Also, due to limited tools in measurements, only the common variables were observed using common methods during experiments.

The main objective was to search for constrain with the current available data and models by considering also explicit salinity impacts on freezing in the model. With the collected data from field, the model was combined with Monte-Carlo sampling method to 1) investigate how well simulated water and solute dynamics corresponded to measured data; 2) identify variability in modeling of water, heat and solute using ensemble simulations; and 3) discuss the influences of solute on soil freezing/thawing based modified freezing point depression function.

2. Material and methods

2.1 Study sites

Studies were conducted at two experimental fields in north China, during 2011/2012, and 2012/2013 wintertime, respectively. One site was located in Qianguo Irrigation District, Songyuan, Jilin (Site NE) (**Fig. 1**). Annual precipitation in Site I was 451 mm and mean monthly air temperature was 5.1 ^{o}C. The study site is typical for its soil texture of clay, which has a high bulk density, low porosity, and low hydraulic conductivity (**Table 1**). The water table in this area fluctuated between 1.5 and 2.0 m. Maximum frost depth in Site I was 1.2 m. In Site I, six plots (2×2 m^2, denoted as P1 to P6) were selected in an agricultural field, which was cultivated with rice from May to October. On 2011/10/09, 20 mm NaBr solution containing 6.5 g L^{-1} Br^- was applied to six plots to form the initial profile for Br^-. Before spraying of the solution, stubbles were removed from the plots and surface was ploughed to depth of 20 cm. Field experiment in Site I was conducted during 2011/2012 wintertime.

The other site was located in Hetao Irrigation District, Inner Mongolia, China (Site IM) (**Fig. 1**). Annual precipitation in this site was 140 mm. Annual mean air temperature 6.4 ^{o}C. Soil texture in this site is characterized as silt loam, with porosity of 0.42~0.46 and saturated hydraulic conductivity of 3.84×10^{-5} m s^{-1}. Water table was kept between 1.5 and 3 m for the winter time, and three irrigation events occur every year in May, July, and November. Soil salt content (mainly NaCl) was 0.1% g g^{-1} for the study field, and irrigation water with electrical conductivity of 0.5 mS cm^{-1}. Before autumn irrigation, five plots (2×2 m^2, denoted as D1-D5) were selected at different parts of the agricultural field, and ploughed to 20 cm depth. Field experiment in this site was conducted during 2012/2013 wintertime.

2.2 Experimental design

TDR probes with 15-cm long and three-rod (CS605) were installed in Site NE to detect liquid water content. A datalogger (TDR 100; Campbell Scientific Inc.) was connected to the probes and recorded daily water data. TDR probes were inserted horizontally into the soil pit (10 m apart from the plots) from 5 cm to 100 cm with 10 cm interval. TDR probes were calibrated in laboratory with unfrozen soil, and the precision was maintained within R^2 of 0.97. PT100 temperature sensors were installed at the same depth as TDR probes, and the daily temperature data was also collected. During soil freezing/thawing, sampling was conducted at 7 dates (2011/10/09, 2011/11/09, 2011/11/25, 2011/12/20, 2012/02/15, 2012/04/10, 2012/04/20), and soil samples from 5 to 100 cm with 10 cm interval were collected for determining total water content and Br^- content. An electric drill (5 cm in diameter, 10 cm in length) was used for sampling soil from depth to depth. Total water content was determined by oven-dry method. Br^- content was determined by diluting 50 g wet soil into 250 mL deionized water, and measuring the electrical potential (mV) using an electrical potential meter (MP523-06). Then the electrical potential was converted into Br^- concentration by a pre-calibrated relationship between Br^- concentration and electrical potential (R^2=0.99). Total water content and Cl^- content in Site IM were sampled at 14 dates (with around 25-d interval) from October 2012 to April 2013 (2012/10/16, 2012/10/27, 2012/11/10, 2012/12/04, 2012/12/15, 2012/12/26, 2013/01/05, 2013/01/14, 2013/01/25, 2013/03/05, 2013/03/14, 2013/03/25, 2013/04/07, 2013/04/18). The sampling and measurement methods for total water content and Cl^- content were the same with those in Site NE. Hourly soil temperatures at 5, 15, 25 and 35 cm depth were recorded by the PT100 temperature sensors from the micro-meteorological station in the field. Groundwater table depth was measured for every 5 d, and the frequency was increased to every 1 d during the autumn irrigation period (2012/11/4 to 2012/11/15). Meteorological data for two sites, e.g., air temperature, humidity, radiation, wind speed, and precipitation, were obtained from the nearest meteorological station with hourly-resolution.

2.3 CoupModel theory

In seasonally frozen soil, the transport of water, heat, and solute in soil profile is coupled with lower boundary (groundwater) and upper boundary (atmosphere) (**Fig. 2**). Water transport processes in CoupModel could be described by combining Darcy's law with mass conservation law:

$$\frac{\partial\theta}{\partial t}=\frac{\partial}{\partial z}\left[k_w\left(\frac{\partial\psi}{\partial z}-1\right)\right]+\frac{\partial}{\partial z}\left(D_v\frac{\partial C_v}{\partial z}\right)-\frac{\partial q_{bypass}}{\partial z} \tag{1}$$

where θ is water content (m^3 m^{-3}); k_w is hydraulic conductivity (m s^{-1}); ψ is matric potential (m); D_v is vapor diffusion coefficient (m^2 s^{-1}); C_v is vapor density (kg m^{-3}); q_{bypass} is the bypass flow in macro pores (m s^{-1}); z is depth to soil surface (positive downward) (m); and t is time (s).

Unsaturated hydraulic conductivity, k_w, is calculated by Mualem equation (Mualem, 1976) combined with Brooks-Corey water retention curve (Brooks and Corey, 1964). Hydraulic conductivity in freezing/thawing soil is modified by dividing water flow domain into high flow and low flow domains (Stähli *et al.*, 1996), and adjusted by using impedance factors, respectively.

Heat flow in soil is described by the heat transport equation, considering conduction, convection and latent heat flow:

$$\frac{\partial(CT)}{\partial t}-L_f\rho_i\frac{\partial\theta_i}{\partial t}=\frac{\partial}{\partial z}\left(k_h\frac{\partial T}{\partial z}\right)-C_wT\frac{\partial q_w}{\partial z}-L_v\frac{\partial q_v}{\partial z} \tag{2}$$

where C is soil (containing solid, water, and ice) heat capacity (J m^{-3} ^{o}C^{-1}); T is temperature (^{o}C); L_f is latent heat of freezing (J kg^{-1}); ρ_i is density of ice (kg m^{-3}); θ_i is ice content (m^3 m^{-3}); k_h is thermal conductivity soil (W m^{-1} ^{o}C^{-1}); q_w is water flux (m s^{-1}); L_v is latent heat of vaporization (J kg^{-1}); and q_v is vapor flux (m s^{-1}).

Thermal conductivity for frozen/unfrozen soil is calculated by the Balland and Arp (2005) method considering the influences of soil components on heat flow.

Solute in CoupModel is considered to transport with water, neglecting diffusion. Solute transport is converted into Cl^- transport in soil:

$$q_{Cl}=c_{Cl}q_w \tag{3}$$

where c_{Cl} is concentration of Cl^- (kg m^{-3}); and q_w is water flux (m s^{-1}).

Upper boundary for model is atmosphere and snow layer is also taken into consideration. Lower boundary is saturated soil layer and drainage is calculated by the combination of empirical drainage equation with Hooghoudt drainage equation The detailed descriptions of water, heat, and solute transport processes as well as model boundaries could be found in the CoupModel manual (Jansson and Karlberg, 2004). Equations used for this simulation work were detailed listed in **Table S2** in Appendix.

2.4 Modification of freezing point depression functions

In CoupModel, the freezing-point depression (**Fig. 3**(a)) is described as below:

Hydrol. Earth Syst. Sci. Discuss., doi:10.5194/hess-2016-507, 2016
Manuscript under review for journal Hydrol. Earth Syst. Sci.
Published: 28 November 2016

$$r = \left(1 - \frac{E}{E_f}\right)^{d_2\lambda + d_3} \min\left(1, \frac{E_f - E}{E_f + L_f w_{ice}}\right) \quad (4)$$

where d_2, d_3 are empirical constants, λ is the pore size distribution index.

In saline frozen soil, ice formation does not start at 0 ^{o}C, but at freezing point of T_0. T_0 is a parameter related to soil type, solute type and solute content. In this approach, T_0 needs to be defined as a parameter in CoupModel, and this parameter could be determined based on experiments or by calibration with soil temperature data for frozen soil. In the present version of CoupModel, T_0 is actually taken as 0 ^{o}C, as shown in **Fig. 3**(a). In this development of the model, T_0 is introduced with values below 0 (from -3 to 0 ^{o}C), the freezing point depression will be like in **Fig. 3**(b).

When calibrating the model in terms of freezing/thawing, parameter T_0 needs to be determined with respect to salt influence on soil freezing/thawing.

As the influence of salt on freezing point is mainly dependent on the osmotic potential of soil solution, a third relationship between freezing point and osmotic potential is built. According to Banin and Anderson (1974), the relationship between freezing point and salt solution could be written as below:

$$T_0 = -1.86c\frac{N_m}{Z} \quad (5)$$

where c is salt concentration (mol L^{-1}); N_m is number of ions to which the salt molecule dissociates; Z is valency of salt.

In CoupModel, osmotic potential (π (cm)) is a function of salt concentration

$$\pi = 10^{-3} \times R(T + 273.15) \cdot c \quad (6)$$

where R is gas constant (8.31 J mol^{-1} K^{-1}); T is temperature (^{o}C); c is salt concentration (mol L^{-1}).

Substituting Equation (6) to Equation (5) will obtain:

$$T_0 = -1.86 \times 10^3 \cdot \frac{N_m}{Z} \cdot \frac{\pi}{R(T + 273.15)} \quad (7)$$

For simplicity, Equation (7) could be expressed as below with a linear relationship between freezing point and osmotic potential:

$$T_0 = -10^{-4+sc} \times \frac{\pi}{1.221} \quad (8)$$

where T_0 is the freezing point (^{o}C); π is osmotic potential (cm); sc is a scale factor for considering the influences of solute types on the relationship (range from -2 to 2); -4 is a constant for converting osmotic potential unit from cm to MPa.

2.5 Uncertainty analysis approach

1) Model performance indicator selection

The likelihood is necessary for a formal objective selection of accepted simulations based on the uncertainty of also the measurement method. However, this requires information about various errors in the measurement approach, which is tricky to obtain without making very extensive investigations. There are many different kinds of substitutes for likelihood functions (Beven and Freer, 2001) when evaluating model performance, and they are widely used in hydrology (e.g., Li *et al.*, 2010; Besalatpour *et al.*, 2012; Pathak *et al.*, 2012). Here, the Nash-Sutcliff index was selected as a performance indicator to be used to reject non-behavioral simulations. This function is calculated as follows:

$$L(\theta\,|\,Y) = \text{NSE}\,R^2 = 1 - \frac{\sum_{i=1}^{N}\left(Y_i - \hat{Y}_i\right)^2}{\sum_{i=1}^{N}\left(Y_i - \bar{Y}\right)^2} \tag{9}$$

where $L(\theta|Y)$ is the indicator for each model run with parameter set θ, N is the total number of measurements, Y_i is the measured value for the ith measurement and $\hat{Y}_i$ is the corresponding output of the model, $\bar{Y}$ is the average of the measured data. If the model predicts the measurements perfectly, we have $Y_i = \hat{Y}_i$, implying $\text{NSE}\,R^2 = 1$. If $\hat{Y}_i = \bar{Y}$ for all i, then $\text{NSE}\,R^2 = 0$ has the same goodness of fit as using the average of the measured data for every situation.

2) Model calibration with Monte-Carlo sampling method

In this work, we calibrated the model in two study sites using data from one winter period within the GLUE framework, respectively. Since this study is to discuss the model performance and parameter uncertainty for a process-based model in simulation of water, heat and solute transport in frozen soils, we would focus more on the calibration of the model instead of validation.

In a physically based model assuming possible variability between soil layers, around 100 parameters are used for simulation. However, for most parameters, they are not necessarily to be calibrated according to the interest of the modeling work. Thus, in this study, a set of parameters that show high sensitivities were selected for calibration, as shown in **Table S1**. These parameters were selected on the basis of one-parameter-at-a-time sensitivity analysis, which was conducted before setting up the model. For the other parameters, they were set as fixed values based on experimental results or references to previous research (Wu *et al.*, 2011a; Gustafsson *et al.*, 2001; Metzger *et al.*, 2015). Then, a uniform prior distribution was assigned to each parameter and 70,000 random parameter sets

Hydrol. Earth Syst. Sci. Discuss., doi:10.5194/hess-2016-507, 2016
Manuscript under review for journal Hydrol. Earth Syst. Sci.
Published: 28 November 2016

Hydrology and Earth System Sciences
Discussions

were created by Monte-Carlo sampling method.

The simulated variables for two sites (temperature, liquid water content at 5, 15, 25, and 35 cm depth for Site NE; temperature, total water content at 5, 15, 25, and 35 cm depth, and groundwater level for Site IM) were compared with mean of measured from multi-plot, and NSE R^2 was used to constrain model performance to achieve the accepted simulations. At Site NE, NSE R^2>0.7 for soil temperature at multi-depth and NSE R^2>-1 for liquid water content at multi-depth were chosen to constrain the simulations. At Site IM, NSE R^2>0.8, NSE R^2>-0.5, and NSE R^2>-0.5 were used for constraining temperature, total water content and groundwater table depth, respectively. These criteria were chosen based on the cumulative distribution of the model performance, by reducing the number of accepted simulations to around 200, and keeping the model performance (NSE R^2) of accepted simulations higher than 80% of all the simulations. Finally, 204 and 222 accepted simulations were obtained for Site NE and Site IM, respectively.

3. Results and discussion

3.1 Water and solute balance analysis

Changes of water and solute storage for different soil horizons showed typical patterns (**Fig. 4**). Seven sampling dates at Site NE divided the whole experimental duration into six periods. While at Site IM, 13 sub-periods were obtained by 14 sampling dates during the experiment. At Site NE, water storage tended to increase from Period 1 to 5 (**Fig. 4**(a)), for 0-10, 0-40, and 0-100 soil zones, except for Periods 2 and 3, when water storage tended to decrease for some zones. For Period 2, water storage decrease in 0-10 cm zone was mainly due to evaporation loss because solute storage (**Fig. 4**(b)) in 0-10 cm zone of this period increased. Besides, solute storage change in three zones during Period 2 were similar, which meant that water and solute change in soil layer lower than 10 cm depth did not influence water and solute storage change in 0-10 cm zone.

Similarly, in Period 3, water loss in 0-10 cm soil layer was also due to evaporation. In Periods 4 and 5, water storage increased largely in soil profile, because of upward movement of water under temperature and potential gradients during soil freezing. In Period 6, water storage in 0-100 cm depth generally decreased, because in this period, soil was thawing, evaporation, runoff would cause large amounts of water loss from soil profile. Solute storage in Periods 5 and 6 showed less change or slight decrease due to loss of water from soil profile.

Water storage at Site NE (**Fig. 4**(c)) generally increased for most periods, with Period 2 for exception. This was because Period 2 is the period when soil was going through extensive evaporation for the fact that water storage at 0-10 cm depth decreased while solute storage (**Fig. 4**(d)) at the same depth increased. Then during the whole winter, water storage in 0-100 cm soil depth kept increasing. Solute storage showed continuous increase in the whole winter-time. Comparing water and storage changes in all three zones for each period, it could be found that changes occurred in the whole soil profile. It was not like that at Site NE, where changes occurred only in the upper layer for some time. This might be due to the climatic differences in two sites during experiments. At Site NE, more precipitation occurred during the winter-time of 2011/2012, which could disturb water and heat as well as solute transport in soil profile due to infiltration of water, snow cover, and re-freezing of soil. The 0-10 cm soil layer at Site NE would be influenced largely by this disturbance and thus show more frequent changes in water and solute storages during experiment. Site IM was characterized as dry winter with sparse precipitation during the experiment. Soil water and solute transport in this site was mainly influenced by the water potential and temperature gradients in soil profile. High groundwater level in this region would also enhance the upward movements of water and solute during winter-time 2012/2013.

3.2 CoupModel performance and parameter uncertainty analysis

Most parameters show similar posterior ranges as the prior ranges (**Table S1**). Large differences between prior and posterior ranges were detected for C_{md} at Site NE, and for ψ_{eg}, s_{def}, $r_{a,max}^{-1}$, $\psi_a(1)$, $\psi_a(3)$, $\psi_a(4)$ at Site IM. The correlations between parameters were normally low, showing that most of the parameters can be taken as independent (**Table S1**). For the parameter showing large differences in prior and posterior range ratios, *NP* was always larger than 1, indicating there were some parameters showing high correlations with it. It should be noticed that the posterior range was obtained based on the substantial improvement of model performance even if the change of most parameters distributions were small. The correlation between parameters should be taken into consideration also when the correlation is low since the combination of many parameters still improved model performance and make interpretation of individual parameters uncertain. However, it does not mean that there must be direct relationships between two parameters with high correlation coefficients. Sometimes the “mass correlation” might exist in statistical analysis work, which means that the correlation between two parameters does not result in the conclusion that the two parameters are connected to each in the model, it is just a statistical result based on large amounts of samples (here the samples are accepted parameter sets).

Thus, a further step of analysis work was conducted (not shown in the study) to plot the scattered relationships between the parameters with correlation coefficients (absolute values) larger than 0.2. Then, the plots were checked one by one based on the scattered relationships and the processes related to these parameters. Finally, 6 parameters in each site were determined as sensitive parameters in calibration, and the cumulative distributions of these parameters are illustrated in **Fig. 5** and **Fig. 6**. For Site NE, the model-sensitive parameters were $r_{a,max}^{-1}$, d_1, $z_{0M,snow}$, C_{md}, s_k, r_{k1}, and they were connected radiation and evaporation process ($r_{a,max}^{-1}$, $z_{0M,snow}$, s_k, r_{k1}) and frozen soil heat process (C_{md}, d_1). For Site IM, the six sensitive parameters belonged to radiation and evaporation process (ψ_{eg}, s_{def}, $r_{a,max}^{-1}$, r_{k1}) and soil water process ($\psi_a(1)$, $\psi_a(4)$), respectively. These parameters showed very different posterior distributions in comparison with the prior uniform distributions, and they showed rapid increase in cumulative probability for certain part of the pre-set ranges.

When looking into the processes that were related to these parameters, it could be found that radiation and evaporation process in both sites seemed to be more sensitive in parameterization. For example, $r_{a,max}^{-1}$ and r_{k1} are two parameters accounting for windless conditions and radiation estimations, respectively. The distributions of these parameters indicated that the proper choice of parameter ranges and distribution related to soil evaporation and radiation process would be of importance in obtaining high model performance. Besides, due to the site-specified conditions in simulation, the specific processes in each site should also be taken into consideration. For example, at Site NE, snow and frost processes showed more sensitive feedbacks with model performance. At Site IM, the water processes in soil and the surface energy balance needed to be taken into account more carefully in calibration of model.

In **Table 2**, the accepted range ratio for model performance for multi-variable is depicted, as well as the number of parameters showing strong correlation with each variable. At Site NE, the accepted ratios for NSE R^2 with respect to all the variables of interest were well constrained to the 50% best, using the selected criteria. The model performance (NSE R^2) for soil temperature at four selected layers was better constrained than total water content and liquid water content at respective layer. This might firstly be due to the fact that soil temperature data was more sufficient (with daily resolution) in comparison with total water content (7 records for each layer) and liquid water content data (around 30 records for each layer). The measurement of soil temperature was automatic with higher precision in comparison with the manual measurement of soil total water content.

Besides, the measurement of liquid water content with TDR was not totally automatic in this study. The measurement was taken at some irregular days by connecting the TDR cables to the datalogger. The measurement of liquid water content with TDR was influenced by a lot of factors, such as soil texture, soil solute and water conditions, these would result in large uncertainties in the data obtained by TDR (Topp *et al.*, 1980; Stähli and Stadler, 1997). The second reason for the poorer performance in modeling water than in temperature was that the water process in frozen soil is much more complex than heat transport, with ice formation, re-freezing and infiltration and drainage considered. These processes are actually influenced by each and result in a high nonlinearity in the model.

The modeling of water and temperature in seasonally frozen soil was reported to have a trade-off, because of the coupled relationships between water and heat transport processes (Wu *et al.*, 2011). At Site NE, the higher precision in temperature data prevailed in obtaining better model performance. It would as a result cause the decrease in model performance for water when constraining the model with selected criteria and aimed size for accepted simulations. For the number of parameters showing strong correlation with model performance of each variable, it could be noted that accepted model performance for each variable was correlated to certain number of parameters in their accepted ranges. This relationship indicated that, when aiming at achieving certain level of model performance for some variables of interest, the parameters related to the processes would be constrained accordingly. They should also be taken into consideration to try to get rid of the condition that one parameter showed opposite feedbacks to variables of different processes or different layers. This would also cause the trade-off between model performance indicators in variables, especially when a multi-objective constraining study was required, both water and temperature were constrained for accepted simulations.

Similarly, at Site IM, the model performance was also well constrained to the 30% best of all the simulations. Soil temperature and total water content model performances were constrained to the 5% best, which were higher than at Site IM. This was mainly because that at Site IM, the soil temperature used for calibration was with 1-h interval recorded data, this would result in a better model performance. The application of criteria for soil temperature model performance would not reduce the number of simulations largely. Even though the total water content data was obtained manually at several dates of the experiment, with relatively large uncertainties, the constraining of total water content model performance would produce reasonable number of accepted simulations. For groundwater table depth, the 23% best of the simulations was obtained, showing good constraining of this variable. Also, several parameters were shown to be tightly related to model performance of each variable,

Hydrol. Earth Syst. Sci. Discuss., doi:10.5194/hess-2016-507, 2016
Manuscript under review for journal Hydrol. Earth Syst. Sci.
Published: 28 November 2016

indicating the complexity and nonlinearity in model, and the uncertainty in obtaining a multi-objective model constraining result.

Fig. 7 shows the modeling results with selected variables in two sites. Uncertainties in measurements and modeling results were added for better understanding of uncertainties in calibration work. Soil temperature at 5 cm depth (**Fig. 7**(a), (d)) show small uncertainties both in measurements and modeling. Total water content at 5 cm depth show relatively large uncertainties in two sites, and larger uncertainties for modeled total water content existed when soil was at the beginning of freezing or end of thawing. Most of the data was obtained when soil was deeply frozen with less water movement in upper layer. This indicated that model parameters might be well constrained for frozen conditions with less water movement. These parameters would not be well applicable for conditions when soil was not frozen deeply with larger water movement in profile or in certain layers. It also implied that it might be good to consider the seasonal characteristics for some parameters for achieving modeling results with consistent performance for the whole period.

In this study, data for non-frozen season was not accessible, further work will be necessary to consider the seasonal patterns in calibration work. When looking into the mean of measured total water content in comparison with modeled mean, total water content at 5 cm at Site IM was generally underestimated by the model, especially for the frozen season (after December). And the range for the measured total water content at 5 cm depth reached as high as 60% cm^3 cm^{-3}, which indicating an over-saturation condition. Eye-inspection during sapling also verified this phenomenon that soil samples at surface layer was detected with some ice-lenses existing, as shown in **Fig. S1**. These ice-lenses would result in large water content in soil and also cause the frost heave in soil profile. This ice-lens at Site IM was mainly due to the intensive irrigation before soil freezing, which maintained high soil water content profile during freezing. When soil began freezing, large amount of water would move upward to occupy the soil pores, and surplus water would accumulate at freezing front, forming the ice lens (Konrad and Morgenstern, 1980; Konrad and Morgenstern, 1981; Watanabe and Mizoguchi, 2000).

Liquid water content at Site NE (**Fig. 7**(c)) was underestimated by the model, in comparison with the measured. This might be due to the fact that, the influence of solutes on freezing/thawing was not taken into account in the model, which would result in a lower modeled liquid water content during soil freezing/thawing. Studies by many researchers (Banin and Anderson, 1974; Stähli and Stadler, 1997; Wu *et al.*, 2015; Wu *et al.*, 2016) have shown that the influences of solutes on soil freezing and thawing should not be neglected in modeling water, heat and solute transport in frozen soil, because the freezing point depression effect was strong. Groundwater table depth at Site IM was also underestimated by the model (**Fig. 7**(f)). In the model, drainage was described by combination of empirical with physical drainage equations. The returning flow was not taken into consideration, as well as the freezing of water in drainage system during the winter. Due to the rapid freezing after irrigation, most of the drained water in the ditches were frozen immediately, and was melted until the end of soil thawing. This would result in a high water level in drainage system, which would make it impossible for efficient drainage during soil freezing/thawing periods. A combination of more detailed agricultural field drainage processes with water body freezing/thawing in cold regions would be of high interest in the future to better predict dynamics of groundwater.

3.3 Uncertainties in water-solute dynamics simulations

Comparison of simulated water storage with measured water storage in different soil profiles is depicted in **Fig. 8**. Results indicated that CoupModel could predict water process well in upper 40 cm soil layer, and some errors occurred for prediction of layer between 40 and 100 cm. This was because the accepted simulations was derived by constraining model performance for variables in upper 40 cm soil layer, and the data from layers lower than 40 cm was not used for validation. This indicated that there might be some other processes in lower layers there were not included in the upper 40 cm layer, and would influence water processes in whole soil profile (from surface to groundwater). Since the model calibration work was focusing on the surface water and energy balance, and the upper layer water process was shown to be well-represented by the model, the more detailed consideration of lower layer water processes exceeded the scope of this study. Further work would be conducted to calibrate the model for the whole soil profile with more detailed measurements.

Fig. 9 shows the simulated salt storage in comparison with measured salt storage based on measured data at various soil layers. For Site NE, the Br^- storage was generally over-estimated by the model in comparison with measured Br^- storage in whole soil profile. Also, the simulated Br^- storage shows larger uncertainty than the measured. Similarly, at Site IM, the simulated Cl^- storage at various layers was larger than measured Cl^- storage. Also, simulated Cl^- storage was shown with larger uncertainty. In the calibration work, only outputs for soil heat (e.g., soil temperature) and soil water (e.g., soil water, liquid water, groundwater) processes were constrained with certain criteria. Due to the assumption of only convection for solute transport in soil, the simulated solute dynamics was tightly related to water dynamics.

However, as could be detected from **Fig. 8**(a), water storage was generally under-estimated for different soil layers. This was in conflict with results from Br^- dynamics. Br^- was added to soil surface before freezing/thawing, and the original Br^- in soil could be neglected. The only changes in Br- storage in each layer could be attributed to transport to or from adjacent soil layers. At Site IM, the Cl^- was used as tracer. Spatial variability in Cl^- caused large uncertainty in measured Cl^- storage at various depths (**Fig. 8**(b)).

As is known that, during soil freezing period the upward of water and solute was the major process. The over-estimation of Br^- storage at various depths indicated that the upward movement of Br^- with water was over-estimated. This might be due to the neglecting of diffusion and repulsion of solute in model. Studies by Cary and Mayland (1972) have shown that, the diffusion and expulsion processes in frozen soil actually played important roles in solute transport even though the convection was the major process. This was because when soil is frozen, soil solution would condense. This would increase solute concentration gradient between frozen layer and unfrozen layer. Also, high solute concentration at low temperature would cause solute expulsion from solution due to low solute saturation. However, it is difficult to obtain the diffusion and expulsion of solute in frozen soil. More detailed experiments on diffusion and expulsion of solute would be of high interest in study of water, heat and solute coupled transport in frozen soils. Large uncertainties in simulated solute storage in both sites indicated that the simulation of solute transport needed to be taken into account more carefully. e.g., more data on solute transport as well as water transport would be of importance in calibration of model, since the water and solute transport processes are tightly coupled in CoupModel.

3.4 Influences of solutes on soil freezing/thawing

In modeling of transport processes in saline frozen soil, the influence of solute on freezing point is also another uncertainty. In CoupModel, the formulation of freezing point depression only takes soil types into consideration, while the solute has shown to be a more important factor in freezing point depression (Banin and Anderson, 1974, Wu et al., 2015). CoupModel takes the freezing point of soil as 0 ^{o}C, which is not reasonable in most agricultural soils because minerals commonly exist in agricultural fields.

In **Fig. 10** and **Fig. 11**, the sensitivity of model results to freezing point depression was analyzed for 5 cm soil layer, based on the proposed freezing point depression functions. The influences of freezing point on soil heat are obvious in **Fig. 10**. Also the model performance was improved by considering freezing point depression due to solute. Mean error (*ME*) for

Hydrol. Earth Syst. Sci. Discuss., doi:10.5194/hess-2016-507, 2016
Manuscript under review for journal Hydrol. Earth Syst. Sci.
Published: 28 November 2016

soil temperature 5 cm depth decreased from 1.25 °C to 0.29 °C at Site NE, and from 2.54 °C to 1.83 °C when freezing point decreased from 0 °C to -3 °C. This indicated that the neglecting of solute effects on freezing/thawing of soil would cause uncertainties in simulation results.

As shown in **Fig. 11**, the relationships between soil temperature and soil heat storage at surface 5 cm layer are different when different values of sc are assigned. *ME* decreased from 1.35 °C to 0.64 °C when sc changed from 0 to 1 for Site NE. For Site IM, *ME* decreased from 2.54 °C when sc is 0 to 2.14 °C when sc is 1. This indicated that in calculation of freezing point, not only the solute content, but also the solute type should also be taken into consideration for reducing uncertainty in modeling soil temperature when soil solute dynamics in frozen soil is not negligible.

In **Fig. 12**, model performance changes in simulating soil temperature at multi-depth were compared before and after adding solute influences on freezing point depression, by using Equation (8). sc was calibrated with ranges from -2 to 2, based on the 204 and 222 calibrated parameter sets with other parameters. The cumulative distribution for NSE R^2 is plotted in **Fig. 12** for comparison. Model performance was improved for different soil depths in both sites, especially for Site NE. This was because at Site NE, only daily mean data was used for calibration of soil temperature. This could cause large uncertainty in simulation of frozen soil. The consideration of solute effects on soil freezing/thawing could improve model performance in simulating heat as well as water processes. This in-turn compensated the uncertainty in inputs. For Site IM, model performance in simulating soil temperature was significantly improved in upper layers (e.g., 5 cm and 15 cm depths). This indicated that detailed description in solute influences on soil freezing/thawing could reduce uncertainty in modeling, and thus improve model performance in modeling surface water and energy balance.

4. Conclusions

Water, temperature and solute during freezing/thawing were simulated and compared with measurements in two seasonally frozen soils in northern China. The uncertainties in both measurements and model were discussed using Monte-Carlo sampling method. Seasonal patterns of water and solute dynamics were detected in both sites during soil freezing/thawing. Water in different soil layers was influenced by both freezing/thawing and evaporation. Solutes tended to accumulate in upper soil layer during the winter. Some model parameters related to radiation/evaporation, soil freezing and snow pack as well hydraulic properties were possible to constrained to a more narrow range based on the applied multi-criterion constraining soil temperature, liquid or total water content and groundwater table. However, trade-off existed between different criteria as well as between different model outputs. Solute has shown to be a key factor influencing soil freezing/thawing. Diffusion and expulsion of solute in frozen soils could result in uncertainties in estimating both water and solute transport with numerical model. Modification of freezing point depression function has shown to be necessary in simulation of mineral-contained soils. Uncertainty in inputs could also be compensated by more reasonable representation of freezing/thawing processes in agricultural soils. CoupModel combined with ensemble simulations method provides an approach for understanding water, heat and solute dynamics as well as parameter uncertainty in seasonally frozen soils. More phenomena like the diffusion and expulsion of solute could not be clarified by the limited amount of data. Detailed experiments on solute transport mechanism would be of high interest in investigation of salinization in cold arid agricultural districts. Future work using more precise measurements and maybe also incorporating more processes into the model are still of high interest in understanding coupled processes in seasonally frozen soil.

Acknowledgements

This research was funded by the National Key Research and Development Program of China (Grant Nos. 2016YFC0501304), National Natural Science Foundation of China (Grant Nos. 51279142, 51379151) and the Twelfth-five National Science and Technology Support Project (No. 2011BAD25B07). We also thank the China Scholarship Council (CSC) for funding this work. We would like to thank Ms. Ai'ping Chen and Mr. Yang Xu from the Yichang Experimental Site for supplying the meteorological data of the studied sites. The authors also appreciate Mr. Pengju Yang, Mr. Dacheng Li and Mr. Weixing Quan for helping analyze the soil samples and processing data in laboratory.

References

Andersland, O.B., Wiggert, D.C. and Davies, S.H., 1996. Frozen soil subsurface barriers: Formation and ice erosion. Journal of contaminant hydrology, **23** (1), 133-147.

Anderson, D.M. and Tice, A.R., 1973. The unfrozen interfacial phase in frozen soil water systems. Ecol. Stud., **4**, 107-125.

Azmatch, T.F., Sego, D.C., Arenson, L.U. and Biggar, K.W., 2012. Using soil freezing characteristic curve to estimate the hydraulic conductivity function of partially frozen soils.

Hydrol. Earth Syst. Sci. Discuss., doi:10.5194/hess-2016-507, 2016
Manuscript under review for journal Hydrol. Earth Syst. Sci.
Published: 28 November 2016

Cold Regions Science and Technology, **83-84**, 103-109.

Baker, G. and Osterkamp, T., 1989. Salt redistribution during freezing of saline sand columns at constant rates. Water Resources Research, **25** (8), 1825-1831.

Baker, J.M. and Spaans, E.J.A., 1997. Mechanics of meltwater movement above and within frozen soil. In: Hanover, N.H. (Ed.), International Symposium on Physics, Chemistry, and Ecology of Seasonally Frozen Soils. U.S. Army Cold Reg. Res. and Eng. Lab., Fairbanks, Alaska, pp. 31-36.

Balland, V. and Arp, P.A., 2005. Modeling soil thermal conductivities over a wide range of conditions. J. Environ. Eng. Sci., **2005** (4), 549-558.

Banin, A. and Anderson, D.M., 1974. Effects of salt concentration changes during freezing on the unfrozen water content of porous materials. Water Resour. Res., **10** (1), 124-128.

Bastola, S., Murphy, C. and Sweeney, J., 2011. The role of hydrological modelling uncertainties in climate change impact assessments of Irish river catchments. Advances in Water Resources, **34** (5), 562-576.

Besalatpour, A., Hajabbasi, M.A., Ayoubi, S. and Jalalian, A., 2012. Identification and prioritization of critical sub-basins in a highly mountainous watershed using SWAT model. EURASIAN JOURNAL OF SOIL SCIENCE (EJSS), **1** (1), 58-63.

Beskow, G., 1947. Soil freezing and frost heaving with special application to roads and railroads.

Beven, K. and Binley, A., 1992. The future of distributed models: model calibration and uncertainty prediction. Hydrological processes, **6** (3), 279-298.

Beven, K. and Freer, J., 2001. Equifinality, data assimilation, and uncertainty estimation in mechanistic modelling of complex environmental systems using the GLUE methodology. Journal of hydrology, **249** (1), 11-29.

Beven, K., 2006. A manifesto for the equilfinality thesis. Journal of Hydrology, **320**, 18-36.

Bing, H. and Ma, W., 2011. Laboratory investigation of the freezing point of saline soil. Cold Regions Science and Technology, **67** (1-2), 79-88.

Black, P.B. and Hardenberg, M.J., 1991. Historical perspectives in frost heave research, the early works of S. Taber and G. Beskow. CRREL Special report.

Brazier, R.E., Beven, K.J., Freer, J. and Rowan, J.S., 2000. Equifinality and uncertainty in physically based soil erosion models: application of the GLUE methodology to WEPP–the Water Erosion Prediction Project–for sites in the UK and USA. Earth Surface Processes and Landforms, **25** (8), 825-845.

Burt, T. and Williams, P.J., 1976. Hydraulic conductivity in frozen soils. Earth Surface

Processes, **1** (4), 349-360.

Cameron, D., Beven, K. and Naden, P., 2000. Flood frequency estimation by continuous simulation under climate change (with uncertainty). Hydrology and Earth System Sciences Discussions, **4** (3), 393-405.

Candela, A., Noto, L. and Aronica, G., 2005. Influence of surface roughness in hydrological response of semiarid catchments. Journal of hydrology, **313** (3), 119-131.

Cary, J. and Mayland, H., 1972. Salt and water movement in unsaturated frozen soil. Soil Science Society of America Journal, **36** (4), 549-555.

Chisanga, C.B., Phiri, E., Shepande, C. and Sichingabula, H., 2015. Evaluating CERES-Maize model using planting dates and nitrogen fertilizer in Zambia. Journal of Agricultural Science, **7** (3), 79.

Choi, H.T. and Beven, K., 2007. Multi-period and multi-criteria model conditioning to reduce prediction uncertainty in an application of TOPMODEL within the GLUE framework. Journal of Hydrology, **332** (3), 316-336.

DeJonge, K.C., Ascough, J.C., Ahmadi, M., Andales, A.A. and Arabi, M., 2012. Global sensitivity and uncertainty analysis of a dynamic agroecosystem model under different irrigation treatments. Ecological Modelling, **231**, 113-125.

Edlefsen, N.E. and Anderson, A.B., 1943. Thermodynamics of soil moisture. University of California.

Flerchinger, G. and Saxton, K., 1989. Simultaneous heat and water model of a freezing snow-residue-soil system I. Theory and development. Trans. ASAE, **32** (2), 565-571.

Flerchinger, G.N. and Saxon, K.E., 1989. Simultaneous heat and water model of a freezing residue-soil system I. Theory and development. Trans. of ASAE, **32** (2), 565-571.

Freer, J., Beven, K. and Ambroise, B., 1996. Bayesian estimation of uncertainty in runoff prediction and the value of data: An application of the GLUE approach. Water Resources Research, **32** (7), 2161-2173.

Groenevelt, P. and Kay, B., 1974. On the interaction of water and heat transport in frozen and unfrozen soils: II. The liquid phase. Soil Science Society of America Journal, **38** (3), 400-404.

Gustafsson, D., Stähli, M. and Jansson, P.-E., 2001. The surface energy balance of a snow cover: comparing measurements to two differentsimulation models. Theoretical and Applied Climatology, **70** (1-4), 81-96.

Gustafsson, D., Lewan, E. and Jansson, P.-E., 2004. Modeling water and heat balance of the boreal landscape-comparison of forest and arable land in Scandinavia. Journal of applied

Hydrol. Earth Syst. Sci. Discuss., doi:10.5194/hess-2016-507, 2016
Manuscript under review for journal Hydrol. Earth Syst. Sci.
Published: 28 November 2016

meteorology, **43** (11), 1750-1767.

Hansson, K., Simunek, J., Mizoguchi, M. and Genuchten, M.T.v., 2004. Water flow and heat transport in frozen soil: Numerical solution and freeze-thaw applications. Vadose Zone Journal, **3**, 693-704.

Harlan, R.L., 1973. Analysis of coupled heat-fluid transport in partially frozen soil. Water Resour. Res., **9**, 1314-1323.

He, J., Jones, J.W., Graham, W.D. and Dukes, M.D., 2010. Influence of likelihood function choice for estimating crop model parameters using the generalized likelihood uncertainty estimation method. Agricultural Systems, **103** (5), 256-264.

Horiguchi, K. and Miller, R.D., 1983. Hydraulic conductivity function of frozen materials. Proc. 4th Int. Conf. Permafrost. National Academy Press, Washington, D.C., pp. 504-508.

Iwata, Y., Hayashi, M. and Hirota, T., 2008. Comparison of Snowmelt Infiltration under Different Soil-Freezing Conditions Influenced by Snow Cover. Vadose Zone Journal, **7** (1), 79. *10.2136/vzj2007.0089*

Iwata, Y., Hayashi, M., Suzuki, S., Hirota, T. and Hasegawa, S., 2010a. Effects of snow cover on soil freezing, water movement, and snowmelt infiltration: A paired plot experiment. Water Resources Research, **46** (9), 1-11. *10.1029/2009wr008070*

Iwata, Y., Hirota, T., Hayashi, M., Suzuki, S. and Hasegawa, S., 2010b. Effects of frozen soil and snow cover on cold-season soil water dynamics in Tokachi, Japan. Hydrological Processes, **24** (13), 1755-1765. *10.1002/hyp.7621*

Jame, Y.W. and Norum, D.L., 1980. Heat and mass transfer in freezing unsaturated porous media. Water Resour. Res., **16**, 811-819.

Jansson, P.-E. and Karlberg, L., 2004. CoupModel: Coupled heat and mass transfer model for soil-plant-atmosphere systems. TRITA-LWR Report 3087. Stockholm, Sweden: Royal Institute of Technology, Department of Land and Water Resources Engineering.

Jones, J.S., 1981. State-of-the-art report—Engineering practice in artificial ground freezing. Engineering Geology, **18** (1), 313-326.

Kay, B. and Groenevelt, P., 1974. On the interaction of water and heat transport in frozen and unfrozen soils: I. Basic theory; the vapor phase. Soil Science Society of America Journal, **38** (3), 395-400.

Khoshkhoo, Y., Jansson, P.E., Irannejad, P., Khalili, A. and Rahimi, H., 2015. Calibration of an energy balance model to simulate wintertime soil temperature, soil frost depth, and snow depth for a 14year period in a highland area of Iran. Cold Regions Science and Technology, **119**, 47-60.

Konrad, J.-M. and Morgenstern, N.R., 1981. The segregation potential of a freezing soil. Canadian Geotechnical Journal, **18** (4), 482-491.

Konrad, J.M. and Morgenstern, N.R., 1980. Heat and mass transfer in freezing unsaturated porous media. Canadian Geotechnical Journal, **17**, 473-486.

Koopmans, R.W.R. and Miller, R., 1966. Soil freezing and soil water characteristic curves. Soil Science Society of America Journal, **30** (6), 680-685.

Lebeau, M. and Konrad, J., 2012. An extension of the capillary and thin film flow model for predicting the hydraulic conductivity of air-free frozen porous media. Water Resour. Res., **48**, W07523.

Li, G., Tiande, M., Hui, Z. and Yonghong, N., 1998. Thermodynamic models of heat moisture migration in saturated freezing soil. CHINESE JOUNAL OF GEOTECHNICAL ENGINEERING.

Li, L., Xia, J., Xu, C.-Y. and Singh, V., 2010. Evaluation of the subjective factors of the GLUE method and comparison with the formal Bayesian method in uncertainty assessment of hydrological models. Journal of Hydrology, **390** (3), 210-221.

Li, N., Chen, B., Chen, F. and Xu, X., 2000. The coupled heat-moisture-mechanic model of the frozen soil. Cold Regions Science and Technology, **31** (3), 199-205.

Li, R., Shi, H., Flerchinger, G.N., Akae, T. and Wang, C., 2012. Simulation of freezing and thawing soils in Inner Mongolia Hetao Irrigation District, China. Geoderma, **173-174**, 28-33. *10.1016/j.geoderma.2012.01.009*

Li, R., Shi, H., Flerchinger, G.N., Zou, C. and Li, Z., 2013. Modeling the effect of antecedent soil water storage on water and heat status in seasonally freezing and thawing agricultural soils. Geoderma, **206**, 70-74. *10.1016/j.geoderma.2013.04.021*

Lin, Y., Wu, W. and Ge, Q., 2015. CERES‐Maize model‐based simulation of climate change impacts on maize yields and potential adaptive measures in Heilongjiang Province, China. Journal of the Science of Food and Agriculture, **95** (14), 2838-2849.

Liu, Y., Freer, J., Beven, K. and Matgen, P., 2009. Towards a limits of acceptability approach to the calibration of hydrological models: Extending observation error. Journal of Hydrology, **367** (1), 93-103.

Lopez, C., Brouchkov, A., Nakayama, H., Takakai, F., Fedorov, A. and Fukuda, M., 2007. Epigenetic salt accumulation and water movement in the active layer of central Yakutia in eastern Siberia. Hydrological Processes, **21** (1), 103-109.

McCauley, C.A., White, D.M., Lilly, M.R. and Nyman, D.M., 2002. A comparison of hydraulic conductivities, permeabilities and infiltration rates in frozen and unfrozen soils.

Hydrol. Earth Syst. Sci. Discuss., doi:10.5194/hess-2016-507, 2016
Manuscript under review for journal Hydrol. Earth Syst. Sci.
Published: 28 November 2016

Cold Regions Science and Technology, **34**, 117-125.

Metzger, C., Jansson, P.-E., Lohila, A., Aurela, M., Eickenscheidt, T., Belelli-Marchesini, L., Dinsmore, K., Drewer, J., van Huissteden, J. and Drösler, M., 2015. CO_2 fluxes and ecosystem dynamics at five European treeless peatlands–merging data and process oriented modeling. Biogeosciences, **12** (1), 125-146.

Miller, R.D., (Ed), 1980. Freezing phenomena in soil. Academic Press.

Mu, S. and Ladanyi, B., 1987. Modelling of coupled heat, moisture and stress field in freezing soil. Cold Regions Science and Technology, **14** (3), 237-246.

Mualem, Y., 1976. A new model for predicting the hydraulic conductivity of unsaturated porous media. Water Resour. Res., **12** (3), 513-522.

Nakano, Y., Tice, A., Oliphant, J. and Jenkins, T., 1982. Transport of water in frozen soil: I: Experimental determination of soil-water diffusivity under isothermal conditions. Advances in Water Resources, **5** (4), 221-226.

Nissanka, S.P., Karunaratne, A.S., Perera, R., Weerakoon, W., Thorburn, P.J. and Wallach, D., 2015. Calibration of the phenology sub-model of APSIM-Oryza: Going beyond goodness of fit. Environmental Modelling & Software, **70**, 128-137.

Parkin, G., von Bertoldi, A.P. and McCoy, A.J., 2013. Effect of Tillage on Soil Water Content and Temperature Under Freeze–Thaw Conditions. Vadose Zone Journal, **12** (1), 0. *10.2136/vzj2012.0075*

Pathak, T.B., Jones, J.W., Fraisse, C.W., Wright, D. and Hoogenboom, G., 2012. Uncertainty analysis and parameter estimation for the CSM-CROPGRO-Cotton model. Agronomy Journal, **104** (5), 1363-1373.

Radke, J. and Berry, E., 1998. Soil Water and Solute Movement and Bulk Density Changes in Repacked Soil Columns as a Result of Freezing and Thawing under Field Conditions. Soil science, **163** (8), 611-624.

Scherler, M., Hauck, C., Hoelzle, M. and Salzmann, N., 2013. Modeled sensitivity of two alpine permafrost sites to RCM‐based climate scenarios. Journal of Geophysical Research: Earth Surface, **118** (2), 780-794.

Seyfried, M. and Murdock, M., 1997. Use of air permeability to estimate infiltrability of frozen soil. Journal of Hydrology, **202** (1), 95-107.

Song, X., Zhang, J., Zhan, C., Xuan, Y., Ye, M. and Xu, C., 2015. Global sensitivity analysis in hydrological modeling: Review of concepts, methods, theoretical framework, and applications. Journal of hydrology, **523**, 739-757.

Spaans, E.J.A. and Baker, J.M., 1996. The soil freezing characteristic: Its measurement and

Hydrology and Earth System Sciences
Open Access
Discussions

similarity to the soil moisture characteristic. Soil Science Society of America Journal, **60**, 205-210.

Stahli, M., Stadler, D., Wydler, H. and Fluhler, H., 2004. Snowmelt infiltration into Alpine soils visualized by dye tracer technique. Artic. Antarctic, and Alpine Research, **36** (1), 9.

Stähli, M., Jansson, P.E. and Lundin, L.C., 1996. Preferential water flow in a frozen soil-A two-domain model approach. Hydrological processes, **10** (10), 1305-1316.

Stähli, M. and Stadler, D., 1997. Measurement of water and solute dynamics in freezing soil columns with time domain reflectometry. Journal of Hydrology, **195** (1), 352-369.

Sun, M., Zhang, X., Huo, Z., Feng, S., Huang, G. and Mao, X., 2016. Uncertainty and sensitivity assessments of an agricultural–hydrological model (RZWQM2) using the GLUE method. Journal of Hydrology, **534**, 19-30.

Topp, G.C., Davis, J.L. and Annan, A.P., 1980. Electromagnetic determination of soil water content: Measurement in coaxial transmission lines. Water Resour. Res., **16**, 574-582.

Wang, X., Frankenberger, J. and Kladivko, E., 2006. Uncertainties in DRAINMOD predictions of subsurface drain flow for an Indiana silt loam using the GLUE methodology. Hydrological processes, **20** (14), 3069-3084.

Watanabe, K. and Mizoguchi, M., 2000. Ice configuration near a growing ice lens in a freezing porous medium consisting of micro glass particles. Journal of Crystal Growth, **213** (1), 135-140.

Watanabe, K. and Flury, M., 2008. Capillary bundle model of hydraulic conductivity for frozen soil. Water Resources Research, **44**, 1-9.

Watanabe, K., Kito, T., Dun, S., Wu, J.Q., Greer, R.C. and Flury, M., 2013. Water Infiltration into a Frozen Soil with Simultaneous Melting of the Frozen Layer. Vadose Zone Journal, **12** (1), 0. *10.2136/vzj2011.0188*

Wettlaufer, J. and Worster, M.G., 2006. Premelting dynamics. Annu. Rev. Fluid Mech., **38**, 427-452.

Wilby, R.L., 2005. Uncertainty in water resource model parameters used for climate change impact assessment. Hydrological Processes, **19** (16), 3201-3219.

Williams, P.J. and Burt, T.P., 1974. Measurement of hydraulic conductivity of frozen soils. Canadian Geotechnical Journal, **11** (4), 647-650.

Wu, M., Tan, X., Huang, J., Wu, J. and Jansson, P.-E., 2015. Solute and water effects on soil freezing characteristics based on laboratory experiments. Cold Regions Science and Technology, **Accepted**. *10.1016/j.coldregions.2015.03.007*

Wu, M., Huang, J., Wu, J., Tan, X. and Jansson, P.-E., 2016. Experimental study on evaporation from seasonally frozen soils under various water, solute and groundwater conditions in Inner Mongolia, China.

Wu, S., Jansson, P.E. and Zhang, X., 2011. Modelling temperature, moisture and surface heat balance in bare soil under seasonal frost conditions in China. European Journal of Soil Science, **62** (6), 780-796.

Wu, S.H. and Jansson, P.E., 2013. Modelling soil temperature and moisture and corresponding seasonality of photosynthesis and transpiration in a boreal spruce ecosystem. Hydrology and Earth System Sciences, **17** (2), 735-749. *10.5194/hess-17-735-2013*

Zhang, W., Wang, G., Zhou, J., Liu, G. and Wang, Y., 2012. Simulating the Water-Heat Processes in Permafrost Regions in the Tibetan Plateau Based on CoupModel. Journal of Glaciology and Geocryology, **34** (5), 1099-1109.

Zhao, Y., Huang, M., Horton, R., Liu, F., Peth, S. and Horn, R., 2013. Influence of winter grazing on water and heat flow in seasonally frozen soil of Inner Mongolia. Vadose Zone Journal, **12** (1).

Zhou, X., Zhou, J., Kinzelbach, W. and Stauffer, F., 2014. Simultaneous measurement of unfrozen water content and ice content in frozen soil using gamma ray attenuation and TDR. Water Resources Research.

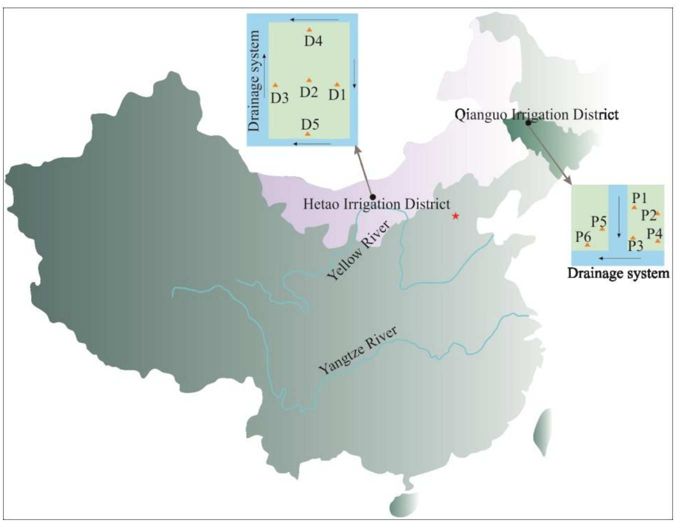

Fig. 1 Study sites layout. P1-P6 denote six sampling plots at Site NE, D1-D5 denote five sampling plots at Site IM.

Hydrol. Earth Syst. Sci. Discuss., doi:10.5194/hess-2016-507, 2016
Manuscript under review for journal Hydrol. Earth Syst. Sci.
Published: 28 November 2016

Hydrology and Earth System Sciences
Open Access
Discussions

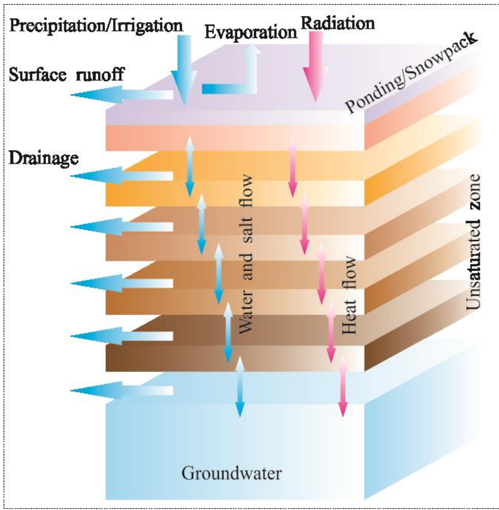

Fig. 2 Structures for CoupModel.

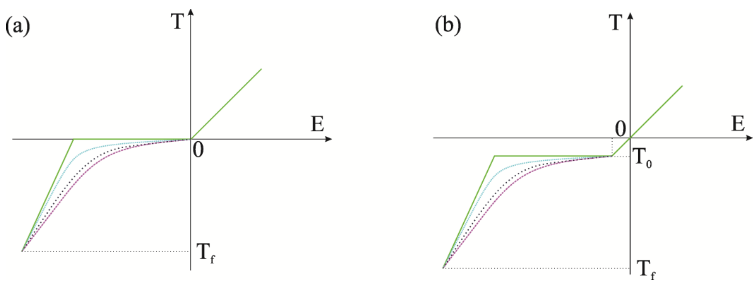

Fig. 3 Modification of the energy-temperature relationship in saline frozen soil.

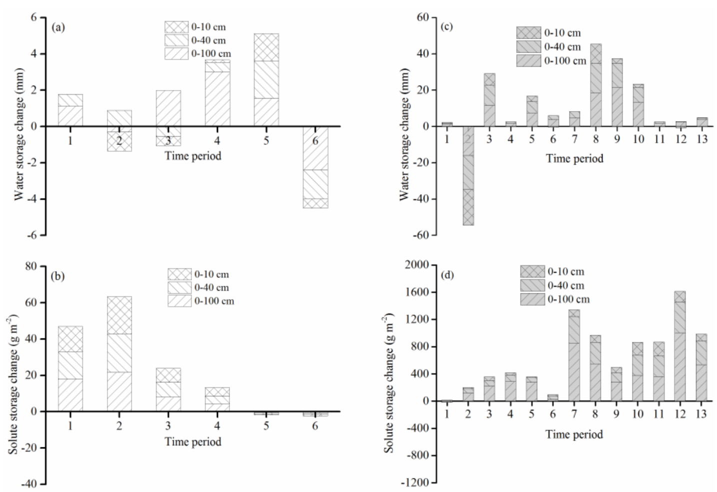

Hydrol. Earth Syst. Sci. Discuss., doi:10.5194/hess-2016-507, 2016
Manuscript under review for journal Hydrol. Earth Syst. Sci.
Published: 28 November 2016

Fig. 4 Mean water and solute storage changes during different periods of soil freezing and thawing at Site NE (a), (b) and Site IM (c), (d). Time period denotes the period during two sampling dates in each site.

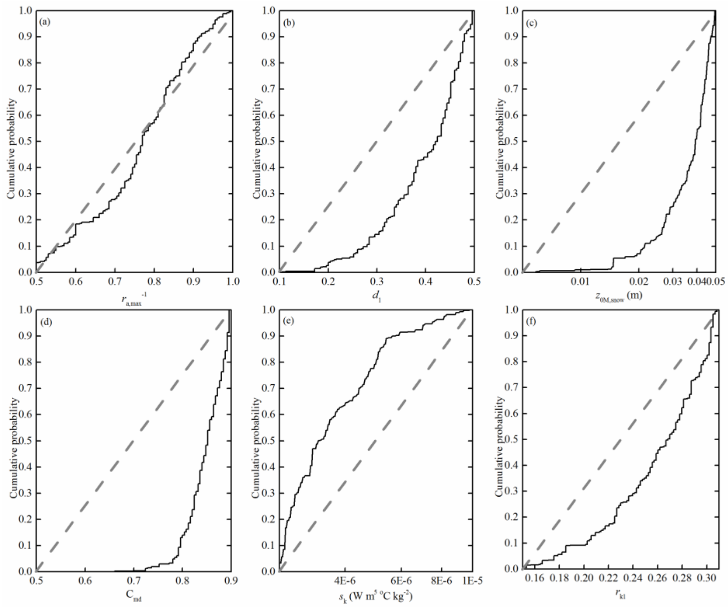

Fig. 5 Cumulative distribution for selected sensitive parameters at Site NE. Grey dashed line denotes prior distribution, and black solid line denotes posterior distribution.

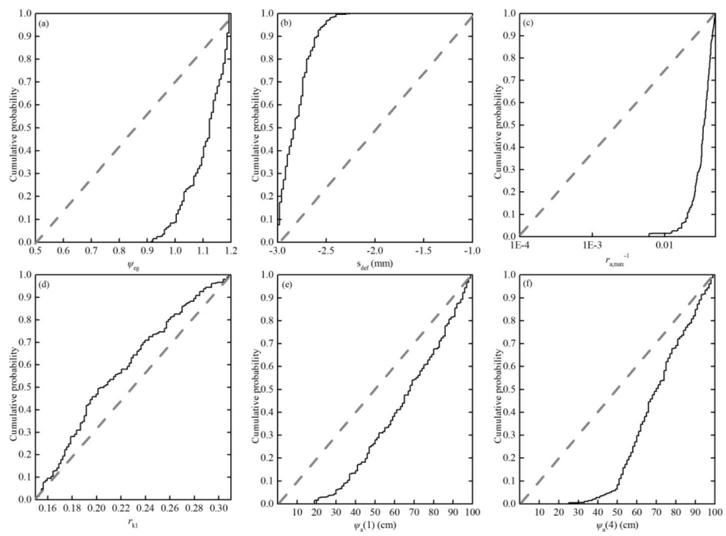

Fig. 6 Cumulative distribution for selected sensitive parameters at Site IM. Grey dashed line

Hydrol. Earth Syst. Sci. Discuss., doi:10.5194/hess-2016-507, 2016
Manuscript under review for journal Hydrol. Earth Syst. Sci.
Published: 28 November 2016

denotes prior distribution, and black solid line denotes posterior distribution.

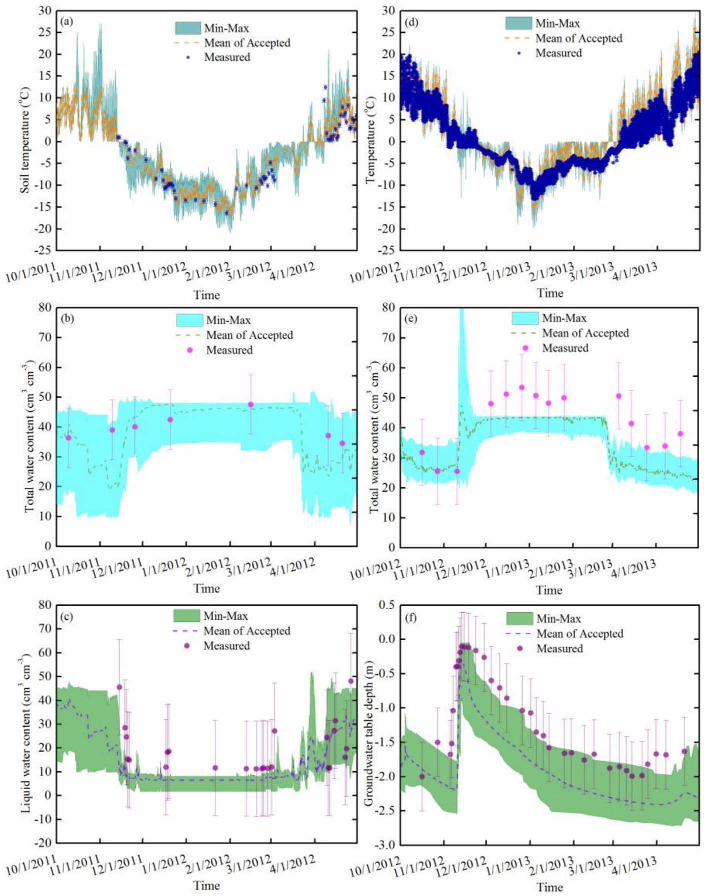

Fig. 7 Comparison of simulated results with measured data in two sites. (a), (b) and (c) are soil temperature, total water content and liquid water content at 5 cm depth at Site NE; (e), (f) and (g) are soil temperature, total water content at 5 cm depth and groundwater water table depth (positive upward) at Site IM. Band shows the accepted range for each variable with minimum and maximum values, and error bar shows the standard error range for all plots.

Hydrol. Earth Syst. Sci. Discuss., doi:10.5194/hess-2016-507, 2016
Manuscript under review for journal Hydrol. Earth Syst. Sci.
Published: 28 November 2016

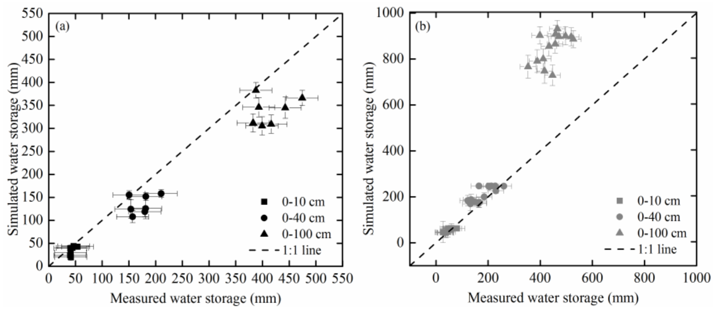

Fig. 8 Comparison of simulated accumulated water storage with measured accumulated water storage in two sites at various soil depths. (a) for Site NE and (b) for Site IM. X and Y error bars denote standard errors for measured and simulated results, respectively.

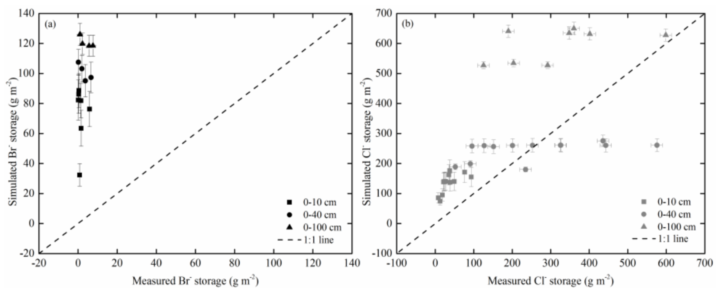

Fig. 9 Comparison of simulated solute storage with measured in two sites. (a) for Site NE and (b) for Site IM. X and Y error bars denote standard errors for measured and simulated results, respectively.

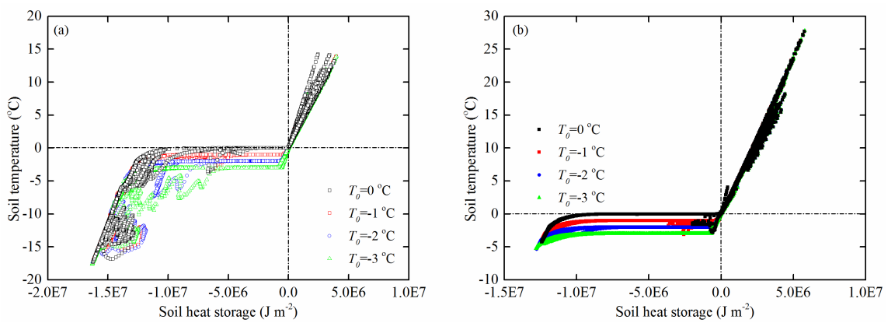

Fig. 10 Relationships between soil temperature and soil heat storage for different freezing point at 5 cm depth at (a) Site NE and (b) Site IM.

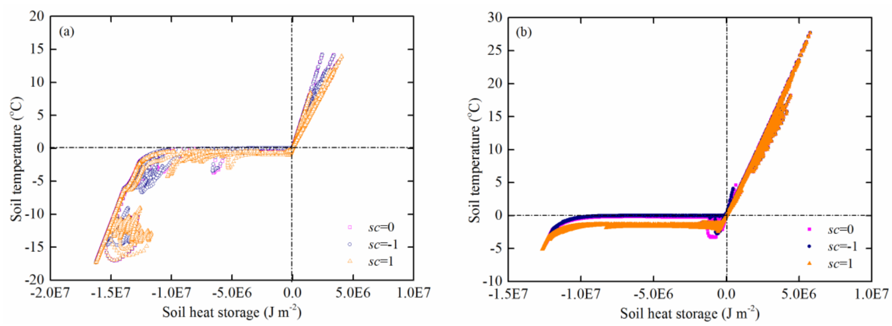

Fig. 11 Relationships between soil temperature and soil heat storage for different *sc* values at 5 cm depth at (a) Site NE and (b) Site IM.

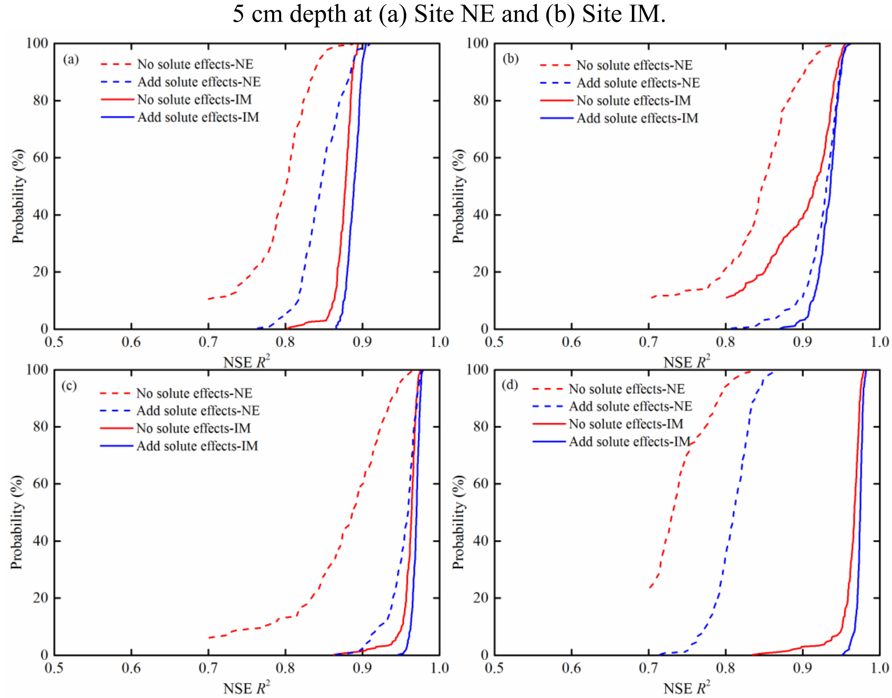

Fig. 12 Comparison of cumulative distribution of NSE R^2 for soil temperature at different soil depths without or with consideration of solute effects on freezing point depression. (a) 5 cm, (b) 15 cm, (c) 25 cm, and (d) 35 cm depths. Red dashed and solid lines denote cumulative distribution of NSE R^2 without consideration of solute effects on freezing point depression with ensemble simulations. Blue dashed and solids lines denote cumulative distribution of NSE R^2 with consideration of solute effects on freezing point depression with ensemble simulations.

Table 1 Soil properties for two sites.

Site	Depth (cm)	Clay (%)	Silt (%)	Sand (%)	Organic matter (%)	CEC (meq/100g)	Bulk density (g/cm^3)	Porosity (-)
NE	0-140	32.40	38.40	29.30	1.76	25.00	1.42	0.46
IM	0-10	27.91	17.20	54.89	1.00	0.50	1.49	0.44
	10-20	37.46	21.65	40.90	1.00	0.50	1.45	0.45
	20-30	31.69	48.39	19.92	1.00	0.50	1.44	0.46
	30-40	34.08	34.32	31.61	1.00	0.50	1.45	0.45
	40-60	28.74	34.85	36.40	1.00	0.50	1.47	0.45
	60-80	34.67	30.45	34.88	1.00	0.50	1.45	0.45
	80-100	17.65	18.46	63.88	1.00	0.50	1.53	0.42
	100-140	14.81	35.05	50.15	1.00	0.50	1.53	0.42

Table 2. Model performance for accepted simulations.

Site name	Site NE						Site IM					
Variable /Depth	Accepted range ratio NSE R^2			^{a}*NP*			Accepted range ratio NSE R^2			*NP*		
	T	θ_t	θ_l	T	θ_t	θ_l	T	θ_t	*GWTD*	T	θ_t	*GWTD*
5 cm	0.24	0.41	0.26	8	4	3	0.02	0.05	0.23	6	5	4
15 cm	0.16	0.35	0.50	4	2	7	0.02	0.05		4	2	
25 cm	0.14	0.29	0.20	6	3	7	0.02	0.03		4	1	
35 cm	0.11	0.31	0.43	3	2	8	0.02	0.02		4	1	

^{a}*NP* denotes number of parameters that show correlation coefficient>0.2 with model performance (NSE R^2).

Hydrol. Earth Syst. Sci. Discuss., doi:10.5194/hess-2016-507, 2016
Manuscript under review for journal Hydrol. Earth Syst. Sci.
Published: 28 November 2016

Hydrology and Earth System Sciences
Open Access
Discussions

Appendix

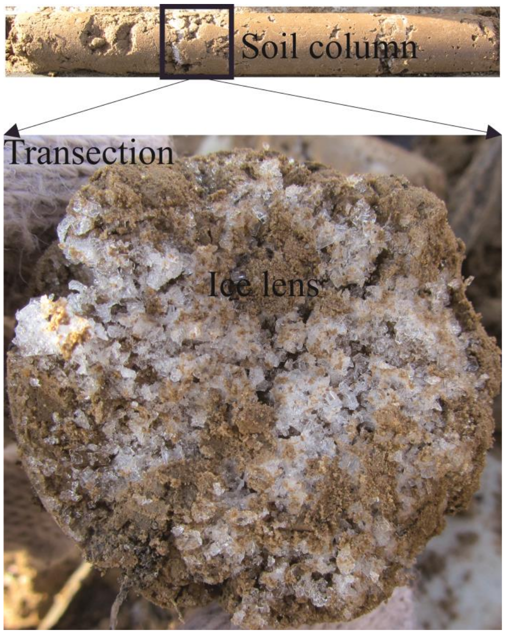

Fig. S1 Ice lens in soil column.

Table S1 Calibrated parameters with ranges and statistical results for posterior.

Name	Symbol	Prior		Posterior Site NE/Site IM		[e]*NP*
		Min	Max	Mean	Range Ratio	
Radiation and evaporation						
AlbedoKExp	k_a	0.5	1.5	1.00 /1.05	1.00 /0.98	0 /0
AlbSnowMin	a_{min}	30	50	37.08 /40.57	0.97 /1.00	2 /0
KonzelmannCoef_1	r_{k1}	0.15	0.31	0.26 /0.21	0.98 /1.00	1 /1
EquilAdjustPsi	ψ_{eq}	0.5	1.2	0.89 /1.11	0.99 /0.40	2 /2
MaxSoilCondens	$e_{max,cond}$	2/[b]1	4/[b]2	2.96 /1.52	0.99 /0.98	0 /0
MaxSurfDeficit	s_{def}	-3	-1	-2.25 /-2.79	0.99 /0.37	0 /1
RoughLBareSoilMom	[a]Z_{0m}	1.0E-05	0.05	0.01 /0.01	0.98 /0.99	1 /0
WindLessExchangeSoil	$r_{a,max}^{-1}$	0.5 /[b]1.0E-04	1 /[b]0.05	0.77 /0.03	0.99 /0.87	7 /2
KBMinusOne	kB^{-1}	0	2.5	0.78 /1.23	0.95 /0.99	2 /0
MaxSurfExcess	s_{excess}	0.5	2	1.26 /1.14	0.97 /0.99	0 /0

Hydrol. Earth Syst. Sci. Discuss., doi:10.5194/hess-2016-507, 2016
Manuscript under review for journal Hydrol. Earth Syst. Sci.
Published: 28 November 2016

Hydrology and Earth System Sciences
Open Access
Discussions

RoughLMomSnow	[a]$z_{0M,snow}$	0.005 /[b]0.025	0.05 /[b]0.05	0.04 /0.04	0.98 /1.00	3 /1
SthermalCondCoef	[a]s_k	2.5E-06 /[b]1.0E-06	1.0E-05 /[b]1.0E-05	3.98E-06 /3.89E-06	0.98 /1.00	2 /0
		Soil heat processes				
CFrozenMaxDamp	C_{md}	0.5	0.9	0.85 /1.05	0.60 /0.98	3 /1
[c]Ballard_Arp Alpha	α	0.1	0.3	0.19 /0.20	1.00 /1.00	0 /0
[c]Ballard_Arp Beta	β	10	30	19.80 /20.07	0.99 /0.99	0 /0
[c]Ballard_Arp a	a	0.4	0.6	0.49 /0.50	0.99 /0.99	0 /0
AlphaHeatCoef	[a]α_h	0.1 /[b]500	5000 /[b]5000	528.40 /2.17E+03	0.97 /0.99	0 /0
FreezepointFWi	d_1	0.1	0.5	0.40 /0.29	0.99 /0.98	2 /0
HighFlowDampC	$c_{\theta,i}$	0.1 /[b]0.1	80 /[b]50	42.00 /25.72	0.98 /0.98	0 /0
LowFlowCondImped	c_{fi}	0.1	10	4.92 /5.05	0.99 /1.00	0 /0
		Soil water processes				
MinimumCondValue	[a]$k_{min\ uc}$	0.0001 /[b]1.0E-06	0.001 /[b]1.0E-05	2.91E-04 /4.18E-06	0.95 /0.98	0 /0
TempFacLinIncrease	r_{A1T}	0.02	0.025	0.02 /0.02	0.99 /0.98	0 /0
Air Entry(1)	ψ_a	0.01	100	50.08 /64.33	0.98 /0.81	0 /1
Air Entry(2)	ψ_a	0.01	100	62.74 /50.78	0.98 /0.92	0 /0
Air Entry(3)	ψ_a	0.01	100	61.84 /64.9	0.98 /0.80	3 /0
Air Entry(4)	ψ_a	[b]0.01	[b]100	-/72.07	-/0.74	-/4
Air Entry(5)	ψ_a	[b]0.01	[b]100	-/38.98	-/0.98	-/0
Air Entry(6)	ψ_a	[b]0.01	[b]100	-/45.73	-/0.99	-/0
Air Entry(7)	ψ_a	[b]0.01	[b]100	-/46.17	-/0.99	-/0
Air Entry(8)	ψ_a	[b]0.01	[b]100	-/43.65	-/0.93	-/0
SurfPoolMax	w_{pmax}	20	100	61.71 /62.14	0.99 /0.99	0 /0
DVapTortuosity	d_{vapb}	0.01	2	0.94 /1.04	0.99 /1.00	1 /1
AScaleSorption	[a]a_{scale}	0.1 /[b]0.02	10 /[b]0.1	2.75 /0.05	0.99 /0.99	1 /0
InitialGroundWater	-	-1 /[b]-2.2	-0.5 /[b]-1.8	-0.76 /-1.99	0.99 /1.00	0 /0
DrainLevel	z_p	-2.5	-2	-2.23 /-2.26	0.98 /0.99	0 /0
DrainLevelMin	-	-1.5	-0.5	-1.04 /-1.00	0.99 /0.98	0 /0
DrainSpacing	d_p	250	300	276.03 /276.23	0.99 /1.00	1 /0
EmpGFLevPeak	z_1	-1.5	-0.5	-0.98 /-0.88	0.99 /1.00	0 /0
EmpGFlowPeak	q_1	5	15	10.19 /9.65	0.99 /1.00	1 /0
		Salt tracer				

Hydrol. Earth Syst. Sci. Discuss., doi:10.5194/hess-2016-507, 2016
Manuscript under review for journal Hydrol. Earth Syst. Sci.
Published: 28 November 2016

SaltInitConc	[a]c_{Cl}	20/[b]800	40/[b]1200	28.10/1004.00	0.99/1.00	0/1
SaltInputConc	[a]c_{Cldep}	1/[b]0.01	10/[b]500	3.87/275.10	0.99/0.98	1/0
SaltIrrigationConc	[a]$c_{Clirrig}$	1500/[b]500	2500/[b]1000	1966.00/756.92	0.99/1.00	0/0
Ad_c(1)	s_{adc}	0	0.5	0.25/0.25	1.00/1.00	0/0
Ad_c(2)	s_{adc}	0	0.5	0.25/0.26	1.00/1.00	0/0
Ad_c(3)	s_{adc}	0	0.5	0.23/0.24	1.00/0.99	0/0
Ad_c(4)	s_{adc}	0	0.5	0.27/0.25	0.99/0.99	0/0
Ad_c(5)	s_{adc}	0	0.5	0.26/0.24	0.99/1.00	0/0
Ad_c(6)	s_{adc}	0	0.5	0.26/0.24	1.00/1.00	0/0
Ad_c(7)	s_{adc}	0	0.5	0.25/0.25	0.99/1.00	0/0
Ad_c(8)	s_{adc}	0	0.5	0.26/0.25	0.99/1.00	1/0
Ad_c(9)	s_{adc}	0	0.5	0.26/0.25	0.99/1.00	1/0
Ad_c(10)	s_{adc}	0	0.5	0.26/0.25	0.99/1.00	1/0
Ad_c(11)	s_{adc}	0	0.5	0.26/0.25	0.99/1.00	1/0
Ad_c(12)	s_{adc}	0	0.5	0.26/0.25	0.99/1.00	1/0
Ad_c(13)	s_{adc}	0	0.5	0.26/0.25	0.99/1.00	1/0
Ad_c(14)	s_{adc}	0	0.5	0.26/0.25	0.99/1.00	1/0
Ad_c(15)	s_{adc}	0	0.5	0.26/0.25	0.99/1.00	1/0
Ad_c(16)	s_{adc}	0	0.5	0.26/0.25	0.99/1.00	1/0

[a]This parameter was sampled using stochastic log distribution, the others using stochastic linear distribution;
[b]Range specific for Site IM;
[c]These parameters are not included into the CoupModel manual (2009), but could be selected in the new version of the model;
[d]Equation is corresponded to the number in CoupModel manual (2009).
[e]*NP* denotes number of parameters showing correlation coefficient >0.2

Table S2 Equations and their descriptions in CoupModel.

No.	Equation	Definition
	Soil water processes	
(E.1)	$q_w = -k_w\left(\frac{\partial\psi}{\partial z}-1\right)-D_v\frac{\partial C_v}{\partial z}$	The total water flow
	where k_w is the unsaturated conductivity, ψ is water tension, z is	

Hydrol. Earth Syst. Sci. Discuss., doi:10.5194/hess-2016-507, 2016
Manuscript under review for journal Hydrol. Earth Syst. Sci.
Published: 28 November 2016

Hydrology and Earth System Sciences
Open Access
Discussions

	depth, C_v is the concentration of vapor in soil air, and D_v is the diffusion coefficient for vapor in the soil.	
(E.2)	$$\frac{\partial\theta}{\partial t}=-\frac{\partial q_w}{\partial z}+s_w$$ where θ is the soil water content and s_w is a source/sink term for e.g. horizontal in the outflow or root water uptake.	Mass conservation equation
(E.3)	$$S_{\text{mat}}=a_{\text{scale}}a_{\text{r}}k_{\text{mat}}\text{pF}$$ where k_{mat} is matric hydraulic conductivity, a_{r} is the ratio between compartment thickness, Δz, and the unit horizontal area represented by the model, pF is $\log_{10}\psi$, a_{scale} is an empirical scaling coefficient accounting for the geometry of aggregates.	Sorption capacity rate estimation
(E.4)	$$D_v=d_{\text{vapb}}f_aD_0$$ where f_a is the fraction of air-filled pores, D_0 is the diffusion coefficient in free air and d_{vapb} is a parameter accounting for tortuosity and the enhancement of vapor transfer observed in measurements compared with theory.	Soil vapor diffusion coefficient
(E.5)	$$S_e=\left(\frac{\psi}{\psi_a}\right)^{-\lambda}$$ where ψ_a is the air-entry tension, λ is the pore size distribution index and S_e the effective saturation.	Water retention curve defined by Brooks and Corey (1964)
(E.6)	$$S_e=\frac{\theta-\theta_r}{\theta_s-\theta_r}$$ where θ_s is the porosity, θ_r is residual water content and θ actual water content.	Effective saturation
(E.7)	$$q_{\text{surf}}=a_{\text{surf}}\left(W_{\text{pool}}-w_{\text{pmax}}\right)$$ where a_{surf} is an empirical coefficient, W_{pool} is the total amount of water in the surface pool, and w_{pmax} is the maximal amount of water stored on	Surface runoff estimation

Hydrol. Earth Syst. Sci. Discuss., doi:10.5194/hess-2016-507, 2016
Manuscript under review for journal Hydrol. Earth Syst. Sci.
Published: 28 November 2016

soil surface without causing surface runoff.

(E.8)	$$k_w = (r_{\mathrm{AOT}} + r_{\mathrm{A1T}} T_s)\max(k_w^*, k_{\mathrm{minuc}})$$ where r_{AOT}, r_{A1T} and k_{minuc} are parameters. k_w^* is the total hydraulic conductivity..	Actual unsaturated hydraulic conductivity after temperature correction
(E.9)	$$k_{fh} = e^{-\frac{\theta_i}{c_{\theta,i}}}\left(k_w\left(\theta_{tot}\right) - k_w\left(\theta_{lf} + \theta_i\right)\right)$$ where $k_w(\theta_{tot})$ is hydraulic conductivity for pores saturated with water; $k_w\left(\theta_{lf} + \theta_i\right)$ is hydraulic conductivity when water flow in low domain with ice existence; $\theta_i / c_{\theta,i}$ is reduced factor; and $c_{\theta,i}$ is impedance factor.	Hydraulic conductivity in high flow domain
(E.10)	$$k_{wf} = 10^{-c_{fi}Q} k_w$$ where c_{fi} is impedance factor; and Q is heat quality.	Hydraulic modification for low flow domain
(E.11)	$$q_{gr} = q_1 \frac{\max\left(0, z_1 - z_{sat}\right)}{z_1} + q_2 \frac{\max\left(0, z_2 - z_{sat}\right)}{z_2}$$ where q_1, q_2, z_1 and z_2 are parameters related to hydro-geological conditions.	Empirical equation for drainage
	Soil heat processes	
(E.12)	$$q_h = -k_h \frac{\partial T}{\partial z} + C_w T q_w + L_v q_v$$ where the indices h, v and w refer to heat, vapor and liquid water, q is flux, k is conductivity, T is soil temperature, C is heat capacity, L is latent heat and z is depth.	Soil heat flow
(E.13)	$$q_h(0) = k_{h0} \frac{(T_s - T_1)}{\Delta z/2} + C_w(T_a - \Delta T_{pa}) q_{in} + L_v q_{v0}$$ where k_{ho} is the conductivity of the organic material at the surface, T_s is the surface temperature, T_1 is the temperature in the upper most soil	Upper boundary condition

Hydrol. Earth Syst. Sci. Discuss., doi:10.5194/hess-2016-507, 2016
Manuscript under review for journal Hydrol. Earth Syst. Sci.
Published: 28 November 2016

layer, ΔT_{pa} is a parameter that represents the temperature difference between the air and the precipitation, q_{in} is the water infiltration rate, q_{vo} is the water vapor flow and L_v is the latent heat.

(E.14)	$$T_{\mathrm{LowB}} = T_{\mathrm{amean}} - T_{\mathrm{aamp}} e^{-\frac{z}{d}} \cos\left(\left(t - t_{ph}\right) w - \frac{z}{d_a}\right)$$ where t is the time, t_{ph} is the phase shift, ω is the frequency of the cycle and d_a is the damping depth, annual mean air temperature, T_{amean}, and amplitude, T_{aamp}, are the parameters.	Lower boundary condition
(E.15)	$$k_{hm} = 0.143\left(a_1 log\left(\frac{\theta}{\rho_s}\right) + a_2\right) 10^{a_3\rho_s}$$ where a_1, a_2 and a_3 are parameters and ρ_s is the dry bulk soil density. The logarithmic argument, $\frac{\theta}{\rho_s}$, is equivalent to the soil water content by weight.	For unfrozen mineral soil an empirical conductivity function
(E.16)	$$k_{hm,i} = b_1 10^{b_2\rho_s} + b_3\left(\frac{\theta}{\rho_s}\right) 10^{b_4\rho_s}$$ where b_1, b_2, b_3 and b_4 are parameters and ρ_s is the dry bulk soil density.	For frozen mineral soil an empirical conductivity function
(E.17)	$$R_f = e^{c_f T_s} c_{\mathrm{md}} + (1 - c_{\mathrm{md}})$$ where T_s is the soil surface temperature and c_f and c_{md} are parameters.	Reduction factor of thermal conductivity in the upper soil layer in frozen soils
(E.18)	$$H = E\left(1 - \frac{L_f w_{\mathrm{ice}}}{E_f}\right)(1 - r)$$ where E is the total energy content in the soil, L_f is the latent heat of freezing, E_f is the total heat content of the soil at the temperature T_f,	Sensible heat content of a partially frozen soil

w_{ice} is the mass of water available for freezing and r is the freezing-point depression.

(E.19) Mass of water available for freezing

$$w_{\mathrm{ice}} = w - \Delta z d_1 \theta_{\mathrm{wilt}} \rho_{\mathrm{water}}$$

where w is the total mass of water, d_1 is a parameter and θ_{wilt} is volumetric water content at a soil water potential corresponding to pF 4.2, and ρ_{water} is the density of water.

(E.20) Freezing-point depression

$$r = \left(1 - \frac{E}{E_f}\right)^{d_2 l + d_3} \min\left(1, \frac{E_f - E}{E_f + L_f w_{\mathrm{ice}}}\right)$$

where d_2 and d_3 are parameters and λ is the pore distribution index.

(E.21) Redistribution of infiltrating water from high flow to low flow domain

$$q_{\mathrm{freeze}} = \alpha_h \Delta z \frac{T}{L_f}$$

where α_h is heat transfer coefficient, Δz is thickness of soil layer, T is soil temperature, L_f is the latent heat of freezing.

Soil evaporation and radiation processes

(E.22) Surface energy balance approach

$$R_n = L_v E_s + H_s + q_h$$

where $L_v E_s$ is the sum of latent heat flux, H_s is sensible heat flux and q_h is heat flux to the soil.

(E.23) Latent heat flux

$$L_v E_s = \frac{\rho_a c_p}{\gamma} \frac{(e_{\mathrm{surf}} - e_a)}{r_{as}}$$

where r_{as} is the aerodynamic resistance, e_{surf} is the vapor pressure at the soil surface, e_a is the actual vapor pressure in the air, ρ_a is the air density, c_p is the heat capacity of air, L_v is the latent heat of vaporization and γ is the psychometric constant.

(E.24) Sensible heat flux

$$H_s = \rho_a c_p \frac{(T_s - T_a)}{r_{as}}$$

where T_s is the soil surface temperature, T_a is the air temperature and

Hydrol. Earth Syst. Sci. Discuss., doi:10.5194/hess-2016-507, 2016
Manuscript under review for journal Hydrol. Earth Syst. Sci.
Published: 28 November 2016

r_{as}, ρ_a, c_p are the same as above.

(E.25) $$q_h = k_h \frac{(T_s - T_1)}{\frac{\Delta z_1}{2}} + Lq_{v,s}$$ Heat flux of the soil

where k_h is the thermal conductivity of the topsoil layer, T_s is the soil surface temperature, T_1 is the middle of uppermost soil compartment temperature, Δz_1 is the depth of the uppermost soil compartment and $Lq_{v,s}$ is the latent water vapor flow from soil surface to the central point of the uppermost soil layer.

(E.26) $$e_{\mathrm{surf}} = e_s(T_s) e^{\left(\frac{\psi M_{\mathrm{water}} g e_{\mathrm{corr}}}{R(T_s + 273.15)}\right)}$$ Vapor pressure at the soil surface

where e_s is the vapor pressure at saturation at soil surface temperature T_s, ψ is the soil water tension and g is the gravitational constant, R is the gas constant, M is the molar mass of water and e_{corr} is the empirical correction factor.

(E.27) $$e_{\mathrm{corr}} = 10^{\left(-\delta_{\mathrm{surf}} \psi_{eg}\right)}$$ Empirical correction factor

where ψ_{eg} is a parameter and δ_{surf} is a calculated mass balance at the soil surface, which is allowed to vary between the parameters s_{def} and s_{excess} given in mm of water.

(E.28) $$\delta_{\mathrm{surf}}(t) = \max\left(s_{\mathrm{def}}, \min\left(\begin{matrix} s_{\mathrm{excess}}, \delta_{\mathrm{surf}}(t-1) + W_{\mathrm{pool}} + \\ \left(q_{in} - E_s - q_{v,s} + i_{\mathrm{drip}}(z_1)\right)\Delta t \end{matrix}\right)\right)$$ Mass balance at the soil surface

where W_{pool} is the surface water pool, q_{in} is the infiltration rate, E_s is the evaporation rate, $q_{v,s}$, is the vapor flow from soil surface to the central point of the uppermost soil layer and s_{def} and s_{excess} are parameters.

(E.29) $$r_{aa} = \frac{1}{k^2 u} \ln\left(\frac{z_{\mathrm{ref}}}{z_{\mathrm{OM}}}\right) \ln\left(\frac{z_{\mathrm{ref}}}{z_{\mathrm{OH}}}\right) f\left(R_{ib}\right)$$ Aerodynamic resistance

where u is the wind speed at the reference height, z_{ref}, R_{ib} is the bulk

Richardson number, k is the von Karman constant and z_{OM} and z_{OH} are the surface roughness lengths for momentum and heat, respectively.

(E.30)	$$kB^{-1} = \ln\left(\frac{z_{\mathrm{OM}}}{z_{\mathrm{OH}}}\right)$$ where kB^{-1} is a parameter with a default value 0 (implies $z_{\mathrm{OH}} = z_{\mathrm{OM}}$).	Equation of kB^{-1}
(E.31)	$$r_{aa} = \left(\frac{1}{r_{aa}} + r_{a,max}^{-1}\right)^{-1}$$ where $r_{a,\max}^{-1}$ is a parameter for a upper limit of the aerodynamic resistance in extreme stable conditions.	Aerodynamic resistance in extreme stable conditions
(E.32)	$$a_{\mathrm{soil}} = a_{\mathrm{dry}} + e^{-k_a^{10}\lg\psi}(a_{\mathrm{wet}} - a_{\mathrm{dry}})$$ where a_{dry} is albedo of dry soil; a_{wet} is albedo of wet soil; and k_a is a transform coefficient from wet to dry soil.	Albedo of bare soil
(E.33)	$$E_s = \max\left(-e_{\mathrm{max,cond}}, L_v E_s / L_v\right) f_{\mathrm{bare}}$$ where $e_{\mathrm{max,cond}}$ is maximum condensation rate for upmost soil layer to maintain water balance.	Soil evaporation limiting factor
(E.34)	$$R_{ns} = R_s(1-\alpha) + R_{nl}$$ where R_s is global radiation; α is albedo of soil; and R_{nl} is net longwave radiation.	Net radiation estimation
(E.35)	$$\varepsilon_{\mathrm{a,Konzelmann}} = \left(r_{k1} + r_{k2}\frac{e_a}{T_a + 273.15}\right)^{1/4}(1-n_c^3) + r_{k3}n_c^3$$ where e_a is vapor pressure; n_c is cloud fraction; r_{k1}, r_{k2}, and r_{k3} are parameters.	Longwave radiation estimation
(E.36)	$$a_{\mathrm{snow}} = a_{\min} + a_1 e^{a_2 S_{age} + a_3 \sum T_a}$$ where $a_{\min}$ is minimum albedo of snow, a_1, a_2, and a_3 are parameter.	Albedo of snow
(E.37)	$$k_{\mathrm{snow}} = s_k \rho_{\mathrm{snow}}^2$$ where s_k is empirical parameter, ρ_{snow} is density of snow.	Thermal conductivity of snow

Hydrol. Earth Syst. Sci. Discuss., doi:10.5194/hess-2016-507, 2016
Manuscript under review for journal Hydrol. Earth Syst. Sci.
Published: 28 November 2016

Hydrology and Earth System Sciences
Open Access
Discussions

(E.38)	$Q_p = \begin{cases} \min\left(1, \left(1 - f_{\text{liqmax}}\right) + f_{\text{liqmax}} \dfrac{T_a - T_{\text{RainL}}}{T_{\text{snowL}} - T_{\text{RainL}}}\right) & T_{\text{a}} \le T_{\text{RainL}} \\ 0 & T > T_{\text{RainL}} \end{cases}$ where f_{liqmax} is parameter, T_{RainL} and T_{snowL} are temperatures above or below which only rain or snow occurs.	Snow thermal quality estimation